PERFACTORY ELECTROLESS RAPID TOOL FOR INJECTION MOULDING

A thesis

submitted in partial fulfilment

of the requirements for the degree

of

Doctor of Philosophy

at

The University of Waikato

by

JANAKA CHANDRAGUPTHA RAJAGURU

———————

The University of Waikato

2015

ABSTRACT

In this research, a rapid tool for low volume production plastic injection moulding is designed, developed, and tested on an injection moulding machine. The tool is designed as a cavity insert of injection mould for plastic parts by an indirect rapid tooling approach. The plastic part is modelled in a CAD system and then built using a Perfactory rapid prototyping (RP) technique. Then a layer of nickel-phosphorous alloy is deposited on the prototype by electroless plating. This nickel plated RP model is then used as a casting pattern. A cavity insert, which is produced by using aluminium filled epoxy resin with the nickel plated casting pattern, is fabricated in a mouldbase for injection moulding. Experimental testing on the cavity insert using an injection moulding machine show that the tool is producing quality parts without any noticeable deterioration of the surface. The number of shots completed using the cavity insert is more than 600.

Applying electroless nickel plating on the casting pattern made of rapid prototyping material was successful. It was found that pre-treatment processes are crucial. In addition, the rapid prototyping material cannot be plated with nickel without palladium activation and stannous sensitising. Results show that the deposited layer is uniform and composed of both nickel and phosphorous. The surface properties of the nickel and phosphorous deposit enhance the plated layer performance due to their low surface roughness and high lubrication characteristics. Moreover, the nickel-phosphorous layer also improves the surface hardness of the cavity insert since it is left on the cavity after the removal of the casting pattern.

The cavity insert was installed on an industrial injection moulding machine for trials. Results show that the cavity insert performs well with Polyethylene at 170˚C at an injection pressure in the range of 80 ~ 100 bar. There are no signs of wear and tear on the cavity insert up to 620 shots. However, when the injection pressure is over 120 bar, cracks start developing in the cavity insert followed by catastrophic fracture.

This research has shown that manufacturing an indirect rapid tooling using electroless nickel plating for low volume production of plastic injection mouldings is feasible for Perfactory produced RP models. The cavity insert can be fabricated using commonly available low cost materials within 48 hours.

ACKNOWLEDGEMENTS

Obviously in a project such as this, there are a number of people who deserve credit. Firstly, I would like to thank my chief supervisor Dr Mike Duke for letting me undertake this work, valuable support and continuing supervision to make the research successful. Also I'd like to thank my co-supervisor Dr ChiKit Au for his thoughts, support and setting me up with a desk and a computer. A very big thank you must also go to my industry mentor, Mark Gasson, for supporting this project and arranging all the prototypes. Thanks must also go to University of Waikato for scholarship funding towards the project.

Also many thanks go to Chris, Martin, Lisa, Helen and other technical staff who help in laboratories and workshops.

Finally, I give thanks to my family members without them I wouldn't have done this.

LIST OF PUBLICATIONS

The following publications have been derived in whole or in part from the work contained within this manuscript. They form the basis of this thesis as well as a body of complimentary work to which the reader may also wish to refer.

Journal Papers:

Rajaguru, J. C., Duke, M. and Au, C.K., 2012, "Study of electroless nickel plating on PerFactory™ rapid prototype model", *Journal of achievements in materials and manufacturing engineering*, Vol. 55, No. 2, pp. 782-789

Rajaguru, J. C., Duke, M. and Au, C.K, 2015, "Investigation of Electroless Nickel Plating on Rapid Prototype Models", *Rapid Prototyping Journal*, (In Press)

Rajaguru, J. C., Duke, M. and Au, C.K, 2015, "Development of rapid tooling by rapid prototyping technology and electroless nickel plating for low-volume production of plastic parts" *The International Journal of Advanced Manufacturing Technology*, Vol. 78, pp. 31-40

Conference Paper:

Rajaguru, J. C., Duke, M. and Au, C.K, 2012, "Study of Electroless Nickel Plating on PerFactory™ R05 Rapid Prototype Model", *Proceedings of 11th Global Congress on Manufacturing and Management*, Auckland New Zealand

TABLE OF CONTENTS

LIST OF FIGURES

LIST OF TABLES

NOMENCLATURE

3D	Three Dimensional
CAD	Computer Aided Design
EDS	Energy Dispersive Spectroscopy
JCPDS	Joint Committee of Powder Diffraction System
MHV	Vickers Micro Hardness
RP	Rapid Prototyping
RT	Rapid Tooling
SEM	Scan Electron Microscope
SLA	Stereolithography Apparatus
SLS	Selective Laser Sintering
STL	Standard Triangular Language
XRD	X Ray Diffraction

Chapter 1: Introduction

1.1 Overview

Recently there is growing interest in the use of rapid prototyping (RP) techniques for rapid tooling and rapid manufacturing applications. This interest is driven by a number of factors including the time and cost for producing parts by conventional manufacturing systems. There are also situations in the manufacturing industry where conventional methods are no longer economical and fast enough to deliver new products to market. In order to shorten the time-to-market and raise the cost effectiveness for product development, increasing research has been directed towards rapid tooling and rapid manufacturing. Both are emerging technologies and many of them adapt from or partially exploit rapid prototyping techniques to develop new approaches to produce tools and parts. The major benefits of both techniques are their cost effectiveness, short time-to-market and least waste in making tools or parts.

1.2 Plastic Part Production

Many manufacturing industries realise how vital it is to launch a new product to the consumer market rapidly. For instance, Hewlett-Packard earned over 80% of its profits from products less than two years old (Jacobs, 1992). The time to develop a car is being reduced from nearly 5 years, 10 years ago, to 1.5 years today (Ding et al. 2003). Hence, it highlights that new products must be developed, manufactured and delivered to the market more quickly and less costly than previously.

Plastic components are incorporated in many products. Mould making for both plastic prototype part development and production component manufacturing is one of the longest and most costly phases in the product development process. Therefore, new technologies such as rapid manufacturing, rapid prototyping and rapid tooling are playing a key role by reducing the time-to-market and making cost effective tooling. These relatively new techniques can be considered as ‘breakthrough’ technologies in the manufacturing industry.

It has been found that in 1999, over 99.99% of all the injection moulds for plastic parts were manufactured either by computer numerical control machining or electrical discharge machining (Hilton, 2000). These are conventional processes for manufacturing moulding tools. These subtractive manufacturing processes are still the dominant manufacturing methods.

Even with the advancement of technology in subtractive manufacturing methods, the tooling process still takes a long time and can be extremely expensive. Six months and US$ 300,000 of investment are not an uncommon initial investment for a moderately complex tool. As a result, the cost per part is rarely economical for low volume production (Hilton, 2000).

Instead of making a tool such as a mould for part production, an additive manufacturing method creates a part directly by adding material layer by layer. After the material particles of one layer are bound by heat or chemicals, the next layer is added and the binding process is repeated. Stereolithography is a typical example of an additive manufacturing method to produce a part. The major advantage of additive manufacturing methods is their low cost for low volume production since an expensive tool is not required in the part production process. Figure 1 shows the variation of cost per part versus the production quality for the injection moulding and stereolithography process respectively.

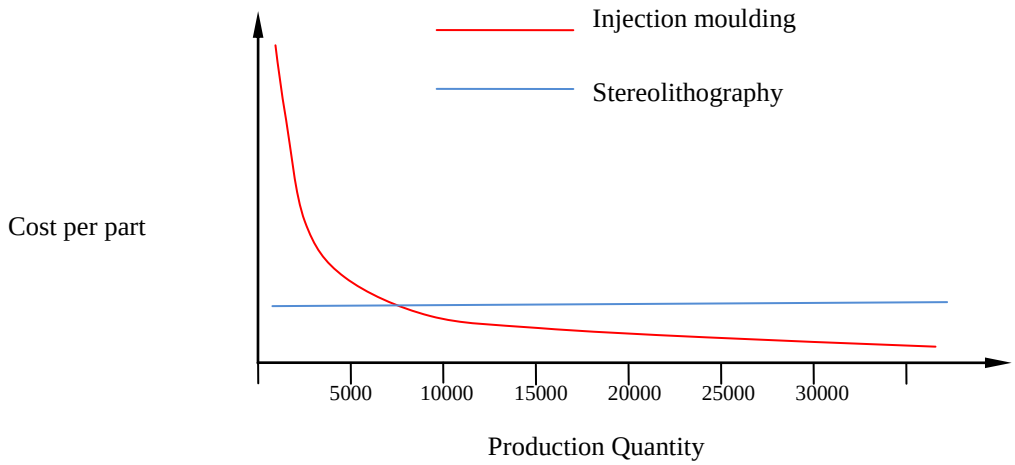

Figure 1: The cost per part versus the production quality for plastic parts (Hilton, 2000)

Referring to Figure 1, conventional injection moulding is economical for high volume production but not viable for low volume production, as cost per part is very high. On the other hand, cost per part produced by stereolithography does not vary with the production volume. Therefore the stereolithography method is more economical for low volume production due to its low cost per part.

However, personalization is one of the trend in product development. This is especially true for medical products. As a result, the plastic parts moulded with high quality at low volume production are not uncommon even though they are components of the same product family. This actually contradicts with having high production volume for injection moulding in order to cut down the manufacturing cost. The aim of this research is to develop a rapid tooling process for building an injection mould quickly and economically for high quality and low volume production of plastic parts.

1.3 Objectives

The objectives of the thesis include:

1. Develop a rapid tooling process to build an injection mould.

A model of the plastic part is printed using the Perfactory RP technique. This model is metalized by plating a layer of nickel on its surface. A cavity insert for injection moulding is created by placing this nickel plated model into aluminium filled epoxy resin. The cavity is then installed into a mould base for production testing.

2. Investigate the properties of the injection mould built by the proposed rapid tooling process.

Both physical and mechanical properties of the nickel plated RP model and the surface of the mould cavity investigated.

3. Investigate the performance and tool life of the injection mould for low volume production.

An injection mould with the cavity manufactured by the proposed approach will be installed in an injection moulding machine for testing. The performance of the injection mould will be investigated during the production process.

1.4 Contribution

The goal of the research is to develop a rapid tooling approach to build an injection mould for low volume production plastic parts. The major contribution of this thesis is to propose a

rapid tooling approach which can shorten the time-to-market and raise the cost effectiveness during the product development process. Technically, the approach proposed in this thesis broadens the application of rapid prototyping technologies to rapid tooling and rapid manufacturing. It also promotes the application of an electroless nickel plating process to a new rapid prototyping material.

Although this rapid tooling approach aims at making the plastic parts for low volume production such as one to two hundred shots, the experimental results show that the injection mould produced by this approach actually has a longer tool life of more than 500 shots.

1.5 Thesis Organization

This thesis consists of seven chapters and the content of each chapter is outlined as follows:

Chapter 2 contains a review of rapid prototyping techniques and rapid tooling for injection moulding. Chapter 3 introduces the proposed methodology to manufacture an injection mould by rapid tooling. Chapter 4 details the process of nickel plating which is a major step in creating the mould cavity. Chapter 5 presents the tests and experiments of the injection mould built by the proposed approach. The life and performance of the tool are also discussed. Chapter 6 discusses various issues and properties of the nickel layer plated on the RP model. Chapter 7 discusses various issues of the proposed approach. Chapter 8 concludes the accomplishment of the research and discusses the future work.

Chapter 2: Literature Review

2.1 Introduction

Rapid prototyping technology is popularly adopted in product development since it can quickly realize the conceptual designs to facilitate the communication among the product development team. In fact, besides getting various designs and manufacturing issues to the surface at the early product development stage, the rapid prototype models can also allow the related product promotion and market activities to start as soon as possible. As a result, rapid prototyping technology is used in many industries such as consumer product, electrical appliances, automobile and even aerospace and aeronautics. Due to the customer requirements, the existing rapid prototyping technologies are largely improved and also getting more and more mature. For instance, the resolution of the model produced by SLA has been greatly improved since it was introduced. At the same time, new technologies and new materials are continuously introduced which yield a higher resolution, more accurate and faster rapid prototyping process. Moreover, these rapid prototyping technologies also advance from product design and development to manufacturing (Jacobs, 1992).

2.2 Rapid Tooling

Rapid tooling is one of the rapid prototyping applications in manufacturing which builds tools quickly and cost effectively for low volume production products. The injection moulding process is commonly employed to make plastic parts in mass production so that the cost per part can be minimized. However, the demand for low volume production of parts is increasing

due to the short time-to-market, high product complexity and diversity. This becomes a driving force to develop a rapid tooling approach to build the injection mould so as to minimize cost and maximize the profit of a product. Therefore, the main requirements for rapid tooling are efficiency, accuracy and cost effective. Various approaches were proposed in the past.

Many authors demonstrated the use of RP for the development of rapid tooling in plastic and wax injection moulding (Sadegh et al., 2009). Kim et al. (2006) reported a rapid tooling method used in a plaster casting process. Rapid tooling can be classified into two groups, namely direct rapid tooling and indirect rapid tooling. They are also referred to as hard and soft tooling. Tools developed using soft materials (i.e. polymers) for short run manufacturing are known as soft tooling. Soft tools are often made from materials like silicon rubber, epoxy resins, low melting point alloys or aluminium. Thus the life of soft tools is low and can only be used in low volume production or intermediate volume production. In contrast, hard tools are usually made of materials such as tool steel and therefore can last a long time and used in high volume production lines.

Direct rapid tooling employs RP technologies to develop tools directly. For example selective laser sintered mould inserts for die manufacturing. Whereas with an indirect rapid tooling method, first a master pattern is generated using a RP technology and then the master pattern is used to develop the required tool. A typical example is fabrication of room temperature vulcanised rubber moulds using SLA master patterns.

Antonio et al. (2010) demonstrated the performance of an aluminium filled epoxy tool built using a rapid prototyping technique. He did not show the number of shots successfully completed by the mould and concluded that an aluminium filled epoxy tool is prone to fast

degradation during the moulding process. However, the cavity insert used in this research shows good wear stability under injection pressure and temperature for more than 600 shots. The reason is the new RT is not just an aluminium filled epoxy tool; it is an aluminium filled epoxy tool with nickel phosphorous layer on it

Rahmati and Dickens (2007) reported on an SLA rapid prototyping, wax injection moulding tool for investment casting. He stated that the tool suffered no damage when subjected to low pressure and temperature wax injection, typically 70˚C and 0.5MPa. The mould had cooling channels and cycle time of 60 seconds.

Ferreira (2004) made a soft tool using rapid prototyping for core boxes used in foundry casting. He made two direct tools using epoxy resin (SLA) and polymeric powder (SLS). He moulded over 100 sand cores from both tools highlighting the time and cost saving. However, the performances of the soft tools were adversely affected by the poor material properties of the polymers and the mould was damaged due to high injection pressure and temperature. However, a nickel-phosphorous alloy layer incorporated in the aluminium filled epoxy resin improved the tool surface and extended the life span of the cavity insert. Furthermore, his research concluded that a soft, rapid tooling mould was not yet a totally satisfactory technology for injection moulding and needed much research and development with new materials to determine the best injection moulding parameters (Ferreira and Mateus, 2000.) This is acceptable as true since there are some operational limitations on the new RT investigated in this research.

Harris et al. (2003) showed that rapid tooling made by SLA epoxy resin has shrinkage of 1% to 2% on the parts depending on the type of material. As a result, it is also expected that this tool also exhibits high part shrinkage compared to conventional moulds. Ma et al. (2007)

prepared an indirect tool from a SLA master pattern and silicon rubber mould. Finally aluminium filled epoxy resin is poured into the silicon mould in order to cast a cavity insert for injection moulding. He successfully produced a part by injection moulding of wax for a short run with the injection pressure and temperature being 70˚C and 2 bar. These pressure and temperature values are relatively low for injection moulding.

Another study by Jorgensen (2001) revealed a SLA direct tool for low volume production of prototypes. Moreover, he stated that the tool had limitations concerning part complexity, fine details and moulding materials since the mould was made from a visco-elastic material which could not withstand high injection pressure and temperature.

Tomori et al. (2004) demonstrated a machined, ceramic filled epoxy tool for low volume production of plastic injection moulding. The tool performed well during the first 150 shots with injection pressure and temperature being 20MPa (200 bar) and 220˚C respectively. That is a good performance as a low volume injection moulding, however this tool was made using conventional machining instead of rapid tooling approach.

Rossi et al. (2004) has applied nickel on to the rapid tooling made by direct metal laser sintering. He made 500 polymeric parts without any defect on the tool. That was a good result for that tool and as it was a metal tool, it should produce more than 500 parts.

Lencina et al. (2007) fabricated an electroless nickel plated SLA rapid tooling for small series production of plastic injection moulding. Results showed that the tool performed better than that without nickel coating and it was sufficient for low volume production injection moulding. No service life of the tool and part complexity was mentioned. Since the tool is made by direct rapid tooling, the whole tool must be electroless plated completely and high adhesive strength between the SLA polymer and nickel-phosphorous alloy is expected.

Harris et al. (2002b) fabricated a direct SLA tool for plastic injection moulding for a small number of parts. The major drawback of the tool was failure in ejecting the parts. The glass transition temperature of the material was reported as 65˚C and the core temperature before starting injection moulding was 55˚C. The mould used in this research was made of aluminium filled epoxy resin with a nickel-phosphorous alloy layer which intends to create less friction and then the phosphorous reducing the risk of failure in ejecting the parts.

Miller (1997) and Derek (2009) reported a CEMCOM nickel shell process. Electroform nickel plated PR is embedded to ceramic mixture and then baked the system to make it harder and melt away the RP materials. The RT produced with CEMCOM also uses nickel plating of a master pattern produced from a RP technique. Steven (1997) says CEMCOM is a promising technique for rapid production of tooling. Still there are many things to improve in the process such as quality, accuracy, stereolithography finishing, devising new ways to cool down parts, etc. In this CEMCOM tool, low thermal conductivity of ceramic leads to longer cycle time or requires an efficient cooling system.

Gibbons and Hansell (2005) demonstrated direct tooling of a steel injection mould insert. It was a direct rapid tooling process that used a laser to melt metal powders layer by layer. Building layer thickness was 100µm and the total mould build time was 32 hours. There was no data on the life of the mould. However, he highlighted the use of rapid prototyping design flexibility to incorporate conformal cooling. The result showed that high part quality was achieved because of good thermal distribution and homogeneity. That tool should be suitable for a long run injection moulding as it is a hard tool. Also 100µm layer thickness should affect the surface quality unless the surface is post treated.

Griffiths, (2013a) demonstrated direct rapid tooling built using a Perfactory mini RP system. The tool was used for low volume production of injection moulded plastic parts. Results showed that the dimensional accuracy was affected by the thermal conductivity when the mould was made from RP material. In fact, he also pointed out that a better understanding of the Perfactory materials are needed in order to improve the results. However in this study, the new tool material is not Perfactory material. It is an indirect tool using master pattern built by Perfactory.

Hopkinson and Dickens (2000) built a SLA rapid tooling and successfully fabricated 50 parts in a sort run plastic injection moulding. The injection pressure was 100bar and nozzle temperature was 185˚C which was a good result for low volume production.

Cheah et al. (2002) developed a rapid tooling using epoxy resin and claimed that the tool life was about 500 parts. Further he stated surface quality and dimensional accuracy is low, moreover cost of the mould making is 5000 USD. In conclusion he stated that for long run production, conventional mould manufacture is still a more suitable choice.

2.3 Motivation

It can be seen that RP materials (or resins) are the most common materials used for direct tooling. Due to the mature development of the RP technologies, tools produced directly from the RP machines can capture all the details of fine features accurately and precisely. However, these RP materials (resins) are soft materials with poor thermal conductivity; they usually cannot withstand the injection moulding processing conditions of high injection pressure and melt temperature. As a result, the tool life can be as short as less than two hundred shots.

Epoxy resins are popular materials in indirect tooling since it is easy to mould with the master pattern. Introduction of metal particles can greatly increase their hardness and thermal conductivity which further improve their tool life. However, the epoxy resins may not capture all the fine features of the master pattern during solidification. Furthermore, the addition of metal particles also causes the epoxy resin mould to changes its brittleness. Therefore, the tool produced by an indirect tooling approach may not last long under injection pressure and temperature.

This research proposes a rapid tooling approach to build a mould for injection moulding efficiently and cost effectively. The approach is also for low to medium volume production of plastic parts. The new RT is not just an aluminum filled epoxy tool. The surface of the tool has an adhesive nickel phosphorous layer lending better results than just an aluminum filled epoxy tool. Replication of model to cavity was done by using a high resolution Perfactory master model. The Perfactory master pattern was nickel plated by electroless nickel since electroforming is not practical as the Perfactory material is non-metallic.

Chapter 3: Research Methodology

3.1 Introduction

Material removal by conventional machining or electric discharge machining are the most expensive and timely processes in injection mould making. These processes are expensive because a high precision computer numerical controlled machine tool is required for accurate material removal. Furthermore, it is also timely to perform the machining processes operation by operation, especially when electric discharge machining is needed since the material is removed particle by particle in micro scale. In order to speed up the manufacturing process and cut down the costs of building a tool for injection moulding, these machining operations should be avoided. The proposed rapid tooling process eliminates the machining processes and make use of the three dimensional printing technology so that the time and costs of manufacturing processes are more effective.

3.2 RT Process

Figure 2 illustrates the concept of the proposed rapid tooling process. The plastic part is designed by CAD software and a RP model of the part obtained by using a 3D printer. This RP model is then used as a casting pattern by implanting into a box of aluminium filled epoxy resin. Most 3D printing materials are resins which are not hard enough for the RP model to be used as a casting pattern. Therefore a layer of nickel is plated on the outer surfaces of the RP model before it is casted into the uncured epoxy resin. Once the epoxy resin has solidified, the RP model is taken out and a cavity insert is formed. Then an injection mould is built by installing the cavity insert into a mould base. Although just a cavity insert is used in this

simple example to illustrate the rapid tooling process concept, the approach can be used for generating both cavity and core side of the insert.

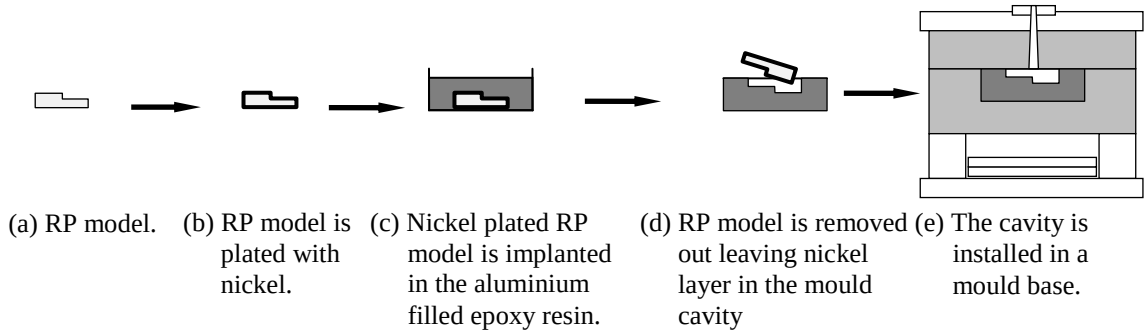

(a) RP model. (b) RP model is plated with nickel. (c) Nickel plated RP model is implanted in the aluminium filled epoxy resin. (d) RP model is removed out leaving nickel layer in the mould cavity (e) The cavity is installed in a mould base.

Figure 2: The proposed rapid tooling approach for building an injection mould.

3.3 RP Model Creation

The cavity insert is built by a casting process. The geometry of the plastic part is modelled by CAD software with all the detail features. The CAD model is then printed by a high resolution 3D printer such as a Perfactory SXGA machine by Envision Tec GmbH. A high resolution 3D printer can print geometric features with dimension of 25μm resolution. In fact, most small features for products like jewellery, toy, and scale models are about 400μm. Figure 3 shows one of the CAD models used as a casting pattern in this research. The overall dimension of the object is ∅20mm×3mm with several small letters on the top face. These letters are either protruded or indented. Since this CAD model will be used as the casting pattern, a draft angle of 4˚ is included.

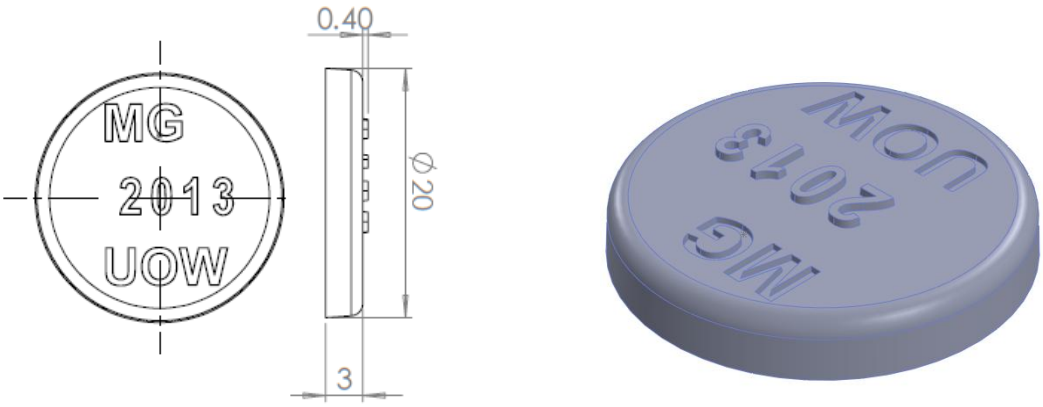

Figure 3: A CAD model and its shaded image.

Most RP materials are proprietary and it is not easy to find their contents and composition. The Perfactory RP material, R5 is a kind of photopolymer. It has very good thermal and mechanical properties compared to other polymer materials (after curing). The material is specially designed for RP applications and is based on specific requirements such as low viscosity, high heat deflection, humidity tolerance, low-curl, dimensional precision and curing behaviour. Some of the properties of R5 Perfactory material are given in Table 1.

Table 1 : Perfactory R5 material properties (EnvisionTEC, 2012)

Property	Measure
Tensile Strength	49.9MPa
Glass Transient Temperature	120 – 50 ºC
Hardness (Shore D)	86
Density	1.215 g/cm^3
Flexural Strength	79.7 MPa

3.4 Nickel Plating of the RP Model

In order to harden the RP model so that it can be used as a casting pattern, a layer of nickel is plated on the outer surface of the RP model by an electroless nickel plating method. Several sub-processes of degreasing, etching, sensitising and activation must be carried out before the plating process. The details of electroless nickel plating of a RP model will be discussed in chapter 4. Figure 4(a) shows a Perfactory RP model and Figure 4(b) shows the same RP model with nickel plating.

(a) Perfactory model (b) Nickel plated Perfactory model

Figure 4: A RP model before and after electroless nickel plating.

3.5 Aluminium Filled Epoxy Mixing and Casting Pattern Implant

Epoxy resin is the most commonly used engineering thermoset material because of its mechanical and thermal properties; high modulus, low creep and elevated temperature performance. Furthermore, reinforced materials can be added into the resin to enhance its mechanical and thermal properties. As a result, it is a popular material for low volume production injection moulding tools.

The epoxy resin used in this research is Z105 with Z206 slow hardener from Adhesive Technologies Ltd. This is Bisphenol A type epoxy resin and relevant hardener. They are mostly used for composite construction and repairs that require high strength, moisture resistance coating, bonding and filling. This resin is filled with aluminium powder as the reinforced material. Aluminium powder was provided by Sigma Alrich and used as received. The aluminium particle size is about 45µm and normally spherical in shape. This small size and low aspect ratio filler enhances the impact resistance of the mixture once cured.

The mixing ratio by weight is 5:1:1 for resin, hardener and aluminium powder respectively. First, epoxy resin and hardener is mixed and stirred thoroughly for few minutes. Then the required amount of aluminium powder is added and stirred thoroughly. This process takes place in a dust free environment at room temperature. The casting pattern is dried before implanting as the moisture has a detrimental effect on the bonding strength of the material. Also, ingress of water into the interface provokes interfacial failure, so care must be taken in handling and storing the aluminium filled epoxy resin in order to avoid water contact and humid environments.

A 90mm Petri dish is placed on a flat table. Then the nickel plated casting pattern is placed at a selected location in the Petri dish. In this case, the centre of circular casting pattern is placed at the centre of the Petri dish. The aluminium filled epoxy resin is quickly poured into the Petri dish until the required depth is achieved. The depth is 11mm in this research. The pouring must be done right after the nickel plating of the casting pattern since nickel oxide will form on the casting pattern which reduces the adhesion to the epoxy resin (Mori et al., 1997).

The Z105 epoxy is a slow curing resin at low temperature. The mixture is allowed to cure at room temperature for 24 hours so that it achieves 90% of its strength. Figure 5 shows the mixture of aluminium filled epoxy resin in the Petri dish.

Figure 5: A mixture of aluminum filled epoxy resin.

3.6 Curing and Machining

The mixture in the Petri dish must not be disturbed during the curing process so that it has enough time to settle and allow for curing reaction to take place. Furthermore, the curing process should be performed at constant temperature. Any temperature fluctuation will lead to sub-optimal mechanical and thermal properties of the resin. It is also important to ensure that the Petri dish is kept upright so that the bottom of the resin is truly horizontal to allow any entrapped air bubbles in the resin to rise up to the top.

Once the resin has solidified, the casting pattern implanted inside is taken out from the Petri dish. Since the bottom of the solidified resin will be the parting face of the injection mould, it needs to be machined to achieve the necessary tolerance as shown in Figure 6.

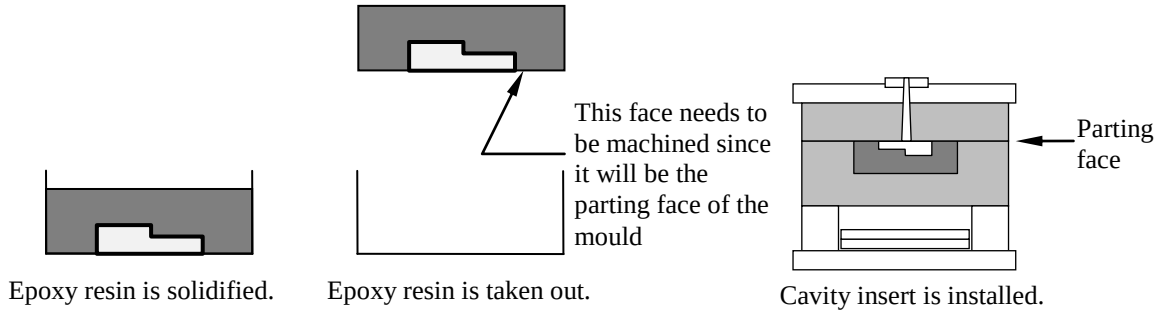

Figure 6: After the curing process.

Extra thickness for machining has to be included when the RP model is designed. For instance, the nominal height of the plastic part is 8.mm. Then the RP model is designed with a height of 8.1mm or 8.2mm. The extra 0.1 ~ 0.2mm is for machining, allowing tight fit so that the cavity insert (which is the solidified epoxy resin with the cavity) seats well when the injection mould is closed. In this research, the solidified epoxy resin is machined by a CY lathe using a standard cutting tool with a spindle speed of 1000rpm. Finally, sand papers with the finest grinding particles are used to polish the face to improve the smoothness.

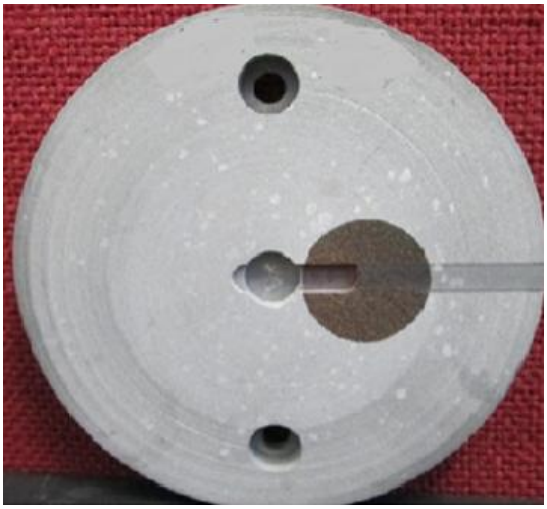

Figure 7: The machined bottom face of a solidified aluminium filled epoxy with the casting pattern implanted.

Figure 7 shows the bottom of a solidified aluminium filled epoxy resin. The dark circular disk is the bottom of the implanted casting pattern. The bottom face of the resin has been machined on a lathe. A runner and a gate are also created. Two small holes are also drilled so that it can be installed in the mould base.

3.7 Casting Pattern Removal

The proposed rapid tooling approach for creating the injection mould is actually quite similar to the investment casting method. In investment casting, the master pattern is burnt out when filling high temperature material (Dvorak, 1998). Furthermore, (Miller, 1997) the master pattern is removed from a mould base by baking the ceramic mould in an oven at high temperature so that the low temperature master pattern melts away. The common removal of the casting pattern from epoxy tools is by using the mould release agent (Dunne et al., 2004b). However, these are not applicable in this case as both the casting pattern and the aluminium

filled epoxy resin have similar glass transition temperatures. In this research, the casting pattern implanted in the aluminium filled epoxy resin is removed thermally.

The solidified aluminium filled epoxy resin is heated to about 65°C which is just around the glass transmission temperature of the RP R5 material and is chiselled away by a mechanical tool. This leaves a cavity replicating the RP model with a layer of nickel compound as shown in Figure 8. This solidified, aluminium filled epoxy resin disc with nickel plated cavity is then ready for installing in the mould base for injection moulding production.

Figure 8: A cavity insert formed by a RP model.

Chapter 4: Electroless Plating of RP Models

4.1 Introduction

Electroless plating is based on autocatalytic chemical reaction in an aqueous media of metal ion to deposit the same ions on an immersion substrate of choice. Nickel salt and a reducing agent are required to perform the process. The nickel ions (Ni^{2+}) are discharged by the electrons (e) which are provided by the reducing agent (R^{n+}). The reactions are expressed as

$$Ni^{2+} + 2e^{-} \rightarrow Ni$$

$$R^{n+} \rightarrow R^{(n+2)+} + 2e^{-}$$

Unlike electro plating, electroless does not need electrical potential to maintain the deposition process so it is a possible plating method for non-metal substrates of complex geometry. Furthermore, the electroless plating process deposits uniform layer irrespective of the substrate geometry. Hence, there is no uneven building up of edges or corners unlike with conventional electroplating. Electroless plating is therefore a good candidate for casting patterns which have small fine features. Therefore, a layer of nickel with uniform thickness on the Perfactory casting pattern (RP model), which has fine features including ribs and recesses, is expected after plating.

The reaction taking place during electroless plating has been investigated since 1946, but till now the electroless plating mechanism has not been fully explained (Malecki et al., 2000). This research is an attempt to get a layer of nickel on the Perfactory casting pattern using an electroless nickel plating process.

The main chemical components in the electroless bath are nickel sulphate as the nickel ion source and sodium hypophosphite as the reducing agent. In addition, both stabiliser agent sodium acetate and pH controller ammonium hydroxide are used. Special attention is given to the plating temperature and pH value because the solution temperature and hydrogen ion H^+ influence the properties and parameters of the electroless plating process and the final deposit. It is important to avoid air bubbles trapped in blind holes or downward facing surfaces. Also the solution is stirred to avoid air bubbles and to make a well mixed solution during plating.

The substrate surface must be catalytic in nature in order to start the reaction. First Palladium acts as a catalyst and initiates the electroless nickel deposition process. Then the deposited layer itself acts as the catalytic surface so that the electroless reaction continues. However, the Perfactory R5 material is a polymer which is a non-metal and is not a catalytic surface for electroless nickel plating. Therefore, special pre-treatment processes of using palladium and stannous is required.

In this research, the substrates for electroless plating are Perfactory RP models which have fine details such as engraved and embossed features. The sizes are as small as 100µm. Figure 9 depicts the processes in electroless nickel plating of Perfactory RP material.

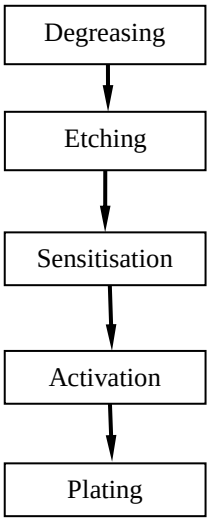

Figure 9: Process in electroless plating of Perfactory material.

4.2 Substrate of the Electroless Plating

Since electroless nickel plating is performed on the casting pattern, the substrate of the plating is the R5 RP material. Figure 10 shows various RP models obtained from the Perfactory machine.

Figure 10: Various Perfactory model for electroless nickel plating.

Firstly, a CAD model of the casting pattern is prepared by using SolidWorks software. The model data in CAD file is translated into machine readable STL (Standard Triangular Language) format and is fed into the Perfactory RP machine. The feature details of the RP model rely on the slicing thickness used to prepare the STL file. The thicker the slicing the higher is the stair effect on the RP model. On the other hand, when the slicing thickness is thin, the machine takes longer time to print the part. Generally, an overall slicing of between 25 µm and 40µm is the most favourable thickness such that the stair effect due to the layer by layer manufacturing system is not visible to the naked eye. Because of the small layer thickness the Perfactory RP model surfaces look very smooth.

Stereolithography is the first commercially available RP technique and is currently widely available in the product development industry. However, the resolution of Perfactory RP

technique is superior to stereolithography. The substrate for electroless nickel plating in this research is a Perfactory rapid prototype model made of photo sensitive acrylic resin with Z direction thickness of 25μm. This resolution can even be used for manufacturing micro moulds. Hence, the stair effect and surface roughness are minimized. Large layer thickness increases crack initiation sites (Rodet and Colton, 2003) so the small layer thickness of Perfactory RP should reduce the possibility of mould cracking.

Because of the small layer thickness, not much post-processing of the Perfactory models is required. In order to improve surface roughness of the final mould surface, the casting pattern surface can be treated with sand blasting to eliminate the stair effect. Sand blasting can yield a surface roughness of 2μm on prototypes (Francis and Haider, 2002). Furthermore, a RP model can be heat treated in a controlled oven to bake the uncured acrylic resin.

4.3 Pre-treatment on Electroless Plating on Perfactory Model

Four processes are required to pre-treat the RP model (which is used as a casting pattern); they are degreasing, etching, sensitizing and activation.

Degreasing

The RP model obtained from the Perfactory machine can be contaminated with dust and grease. Since electroless nickel plating depends on the surface of the RP model, cleaning is important as contaminants on the surface lead to uneven surface roughness and loss of adhesion. Therefore, the Perfactory model is degreased by sodium hydroxide (NaOH). The solution concentration is 20g/l which is a usually adopted concentration for degreasing plastics. The model is immersed in a beaker of sodium hydroxide (NaOH) solution and is

allowed to soak for 5 minutes at room temperature. Then it is rinsed with distilled water followed by air drying.

Etching

After the RP model is degreased, all the surfaces of the RP model (which will be the substrate for plating) are etched with sulphuric acid (H_2SO_4) and chromic acid solution (CrO_3). The degreased RP model is immersed in a chromic acid solution for 5 minutes at room temperature. After that it is rinsed with distilled water followed by drying. CrO_3 concentration is 1g/l for 20ml of 98% sulphuric acid in 1 litre of distilled water.

One common etching method to raise the hydrophilicity of the substrate is to maintain the solution bath temperature at 65-70 ˚C and a trace amount of metal ion such as palladium ion Pd^{2+} is added for plating plastic parts in order to enhance the etching effect and increase the etching rate (Luan et al., 2000). However, in this research, the etching process for R5 RP material is performed at room temperature (instead of 65^0C ~ 70^0C) using a chromic acid solution and the etching process is successful.

The Perfactory photopolymer R5 material after curing has good chemical resistance. Hence, although the sulphuric acid is very corrosive; it is a good agent for etching. Moreover, when the sulphuric acid is mixed with chromic acid, the etching effect is even improved. The treatment oxidises the substrate surface strongly and forms polar radicals to improve hydrophilicity and surface roughness (Di et al., 2011). Furthermore, employment of the chemical etching improves the adhesion of nickel deposition on to the substrate (Waris et al., 2005).

Sensitizing

Sensitizing is to seed such a strong chemical like tin ions Sn^{2+} in the RP model surface to reduce activating metal ions. This uniform seeding layer of tin ions Sn^{2+} is to react with palladium ions Pd^{2+} in the next step. Under sensitization, the substrate is wetted by immersing it in a stannous chloride ($SnCl_2$) solution for 1 minute followed by washing with distilled water.

Activation

Various activation processes are found for electroless plating on plastics (Tang et al. 2008 and 2011). In this research, a classical and conventional activation method is adopted. There is no data from past research regarding activation of Perfactory R5 photopolymer. All the surfaces of the substrate are activated by dipping in a palladium chloride ($PdCl_2$) solution for 5 minutes.

$$Pd^{2+} + Sn^{2+} \rightarrow Sn^{4+} + Pd^{0}$$

Both stannous chloride and palladium chloride solutions are prepared by dissolving them in a hydrochloric acid solution (HCl). Once palladium is seeded on to the casting pattern then it is ready for plating. The palladium acts as a catalyst on the R5 photopolymer surface to initiate electroless plating when the substrate is immersed in the electroless plating solution. Furthermore, the palladium seeded layer is the media for adhesion between the substrate and deposit. The load transferring capacity is improved (Li et al., 2011).

The bath composition of bath solutions used for pre-treatment and the reaction conditions are listed inTable 2.

Table 2: Bath composition of pre-treatment solutions.

Solution Name	Composition of the solution	Condition
Etching	Chromic Acid	1g/l
	Sulphuric Acid (98%)	370g/l
	Temperature	Room temperature
Sensitizing	Tin (II) Chloride	1g/l
	Hydrochloride Acid (36%)	3.567g/l
	Temperature	Room temperature
Activation	Palladium Chloride	0.1g/l
	Hydrochloride Acid (36%)	11.89g/l
	Temperature	Room temperature
	Immersion time	5 min

4.4 Plating

Electroless nickel plating can be executed in either acidic or alkaline solution. Both solutions follow the same redox reaction while the surface and structural properties of the nickel layer are different (Cheon et al., 2011).

Alkaline type electroless nickel plating is adopted in this research. An alkaline electroless solution of nickel sulfatehexahydrate ($NiSO_4.6H_2O$) and sodium hypophosphite (NaH_2PO_2) with a pH value over 7 are used. In this bath, sodium hypophosphate serves as a reducing agent and nickel sulphate provides metal ions. Other chemicals include sodium acetate and sodium citrate dehydrate to work as a stabiliser agent and a buffer agent.

The electroless nickel plating is performed in an alkaline solution since it yields better adhesion of nickel deposited on the RP model. Moreover, it also improves the plating rate if the plating is performed at a higher temperature. The RP model is immersed into the electroless solution at a temperature of 80°C. The solution pH value is maintained at 10. The experimental setup is placed inside a fume hood and is set to run by mixing sodium hypophosphite as shown in Figure 11.

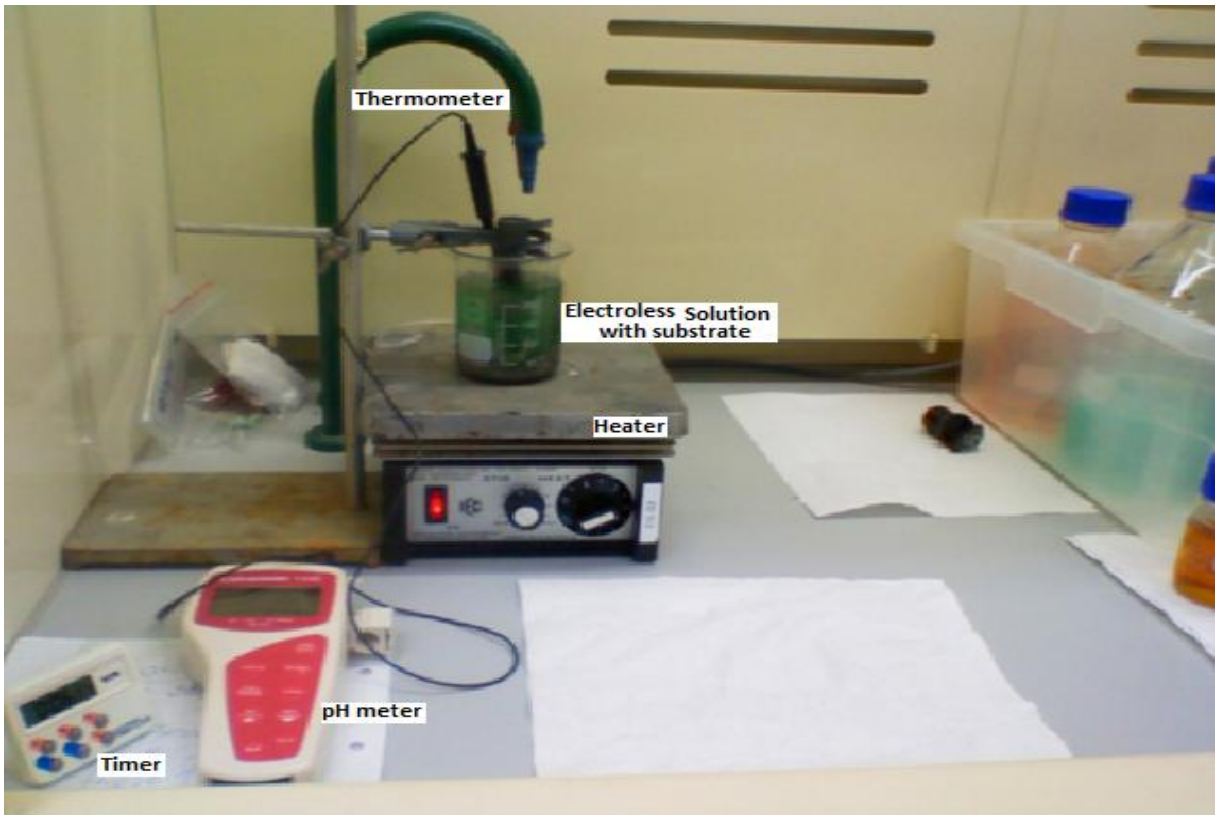

Figure 11: Experimental setup for electroless nickel plating on RP material.

Table 3: Chemical compositions and conditions for the electroless nickel plating.

Chemicals	Concentration	Condition
$NiSO_4.6H_2O$	20g/l	80 °C , pH 10, deionised water
$NaH_2PO_2{\cdot}H_2O$	20g/l	80 °C , pH 10, deionised water
$Na_3C_6H_5O_7{\cdot}2H_2O$	11.4g/l	
CH_3COONa	10g/l	
H_2SO_4	98%	Sigma Aldrich, used as received
H_2O		Room temperature, deionised water

After many attempts and variations, Figure 12 shows the first successful plating result. The shark model is printed by a Perfactory RP machine with R5 RP material. The nickel deposition starts immediately after the pre-treated RP model is partially immersed into the electroless solution. The plating time is about one hour. Figure 12(a) shows the nickel depositing on the RP model when it is just taken out from the bath. Figure 12(b) shows the model after rinsing. The tail of the shark model is taken away from the plated model for mechanical properties examination.

(a) The RP model is taken out from the bath.

(b) The RP model after rinsing by de-ionized water.

Figure 12: Experimental result of electroless nickel plating on R5 RP material.

Figure 13 shows the electroless nickel plating result of another RP model. All the surfaces become silver grey and opaque when the nickel compound layer is introduced. Moreover, the plated surfaces are smooth and matte. The engraved and embossed features on the model are very clear and there is no effect on the dimensional accuracy of the models as the layer is micro thin. There are also no visible signs of bubbles or peel off segments in the plated nickel deposit.

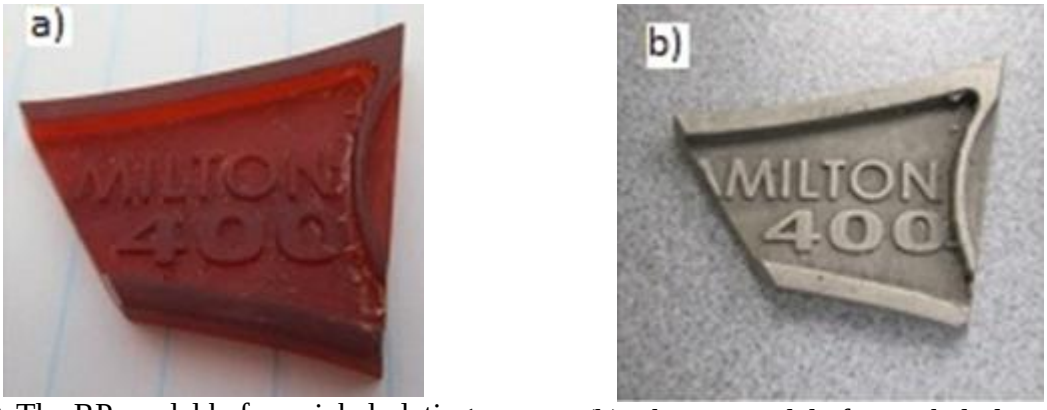

(a) The RP model before nickel plating. (b) The RP model after nickel plating

Figure 13: Experimental result of electroless nickel plating on the other R5 RP models.

Eventually an electroless nickel layer was obtained on the Perfactory R5 polymer material surface. The layer of nickel was achieved after many experiments. Many times it failed to get any deposit. There may be many reasons as to why a deposit cannot be achieved in the Perfactory models, for example, incorrect chemical composition of pre-treatment processes, not enough etching effect and problems in activation. Sometime the deposit is defective. The deposit is not uniform and cracks in the deposit were seen. Again the reasons behind those could be problems in pre-treatment and plating temperature. Eventually, a well-defined and reliable process was developed that enabled consistent, good quality nickel plating of Perfactory RPs.

Chapter 5: Experimental Analysis of the Deposited Ni-P on RP Material

5.1 Introduction

Electroless nickel plating is a popular process to deposit a layer of nickel on tools in many industrial applications. The nickel layer can protect a tool from wear and is therefore well suited to injection moulding. The properties of the nickel layer depend on various process parameters of the electroless plating process, pre-treatment process, substrate materials and surface quality.

The tests listed in Table 4 have been conducted using relevant instruments to investigate the properties of the nickel layer which is plated on the R5 rapid prototyping material by electroless plating. Sample preparations according to the relevant machine and test requirements are also explained.

Table 4: Investigation on various properties of nickel layer plated on RP material by electroless plating

Instruments	Properties
Scanning electron microscope	Surface Morphology
Optical microscope	Surface Visualisation
Energy dispersive spectroscopy	Chemical Composition of deposit
X-ray diffraction	Ni-P Structure
MVH	Hardness

5.2 Pre-treatment Process

The RP R5 material is a non-metal and it does not attract the nickel ions during the electroless nickel plating process. As a result, the process is not auto-catalytic. In order to restore the nickel ion attraction on the substrate, preliminary treatments are necessary. The treatments include sensitization and subsequent activation of the RP material by using the following solutions: sodium hydroxide, chromic acid, stannous chloride and palladium chloride.

The surface morphologies of the RP model during pre-treatment are investigated using Hitachi S4700 scanning electronic microscopic (SEM) and are shown in Figure 14. During the degreasing process, there is no significant difference in the RP model surface morphology compared to the original surface as shown in Figure 14(a) and Figure 14(b). The etching process is performed by chromic acid which makes the substrate hydrophilic so that it can be wetted by the stannous chloride. After etching, the surface shown in Figure 14(c) exhibits an oxidized rough morphology which consists of some pits. That is similar to the situation of increasing surface area by introducing holes (Alexandre et. al. 2010). Those pits are generated due to the selective corrosion by sulphuric acid which enhance the seeding area for stannous and palladium ions. Furthermore, those pits also act as anchor points to adhere the final nickel layer to the substrate which yield a high degree adhesion layer to the RP model. A 1000× magnification image of the surface after etching is shown in Figure 14(d).

The substrate is sensitized by absorbing the tin (Sn^{2+}) ions from stannous chloride solution which reacts with the palladium (Pd^{2+}) ions during the activation process. The electroless nickel plating cannot be activated without seeding of the palladium ions on the substrate surface. After sensitizing and activation, there is no significant morphology change as shown

in Figure 14(e). The morphology of the final phase after electroless plating is shown in Figure 14(f).

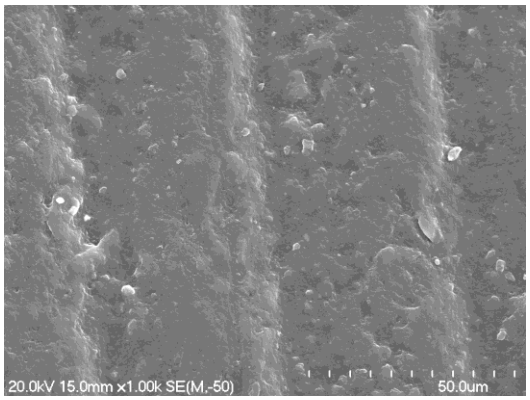

(a) Original RP model surface.

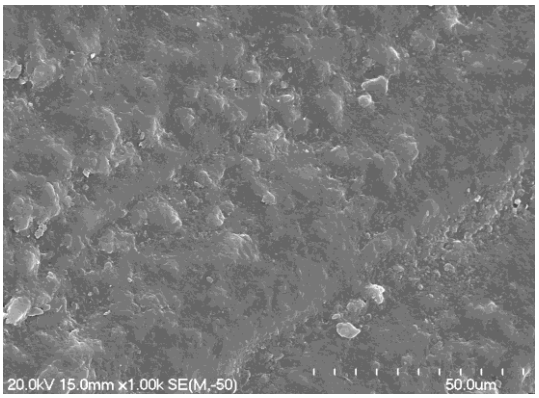

(b) Surface after degreasing.

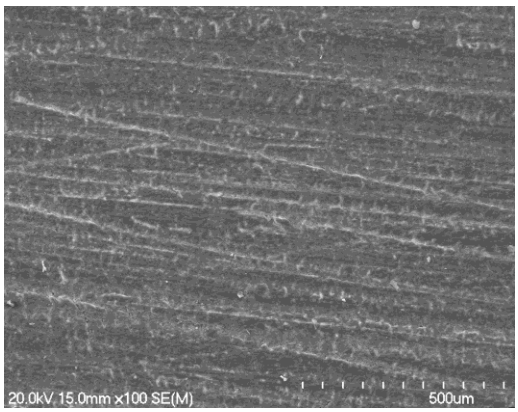

(c) Surface after etching at 100× magnifications.

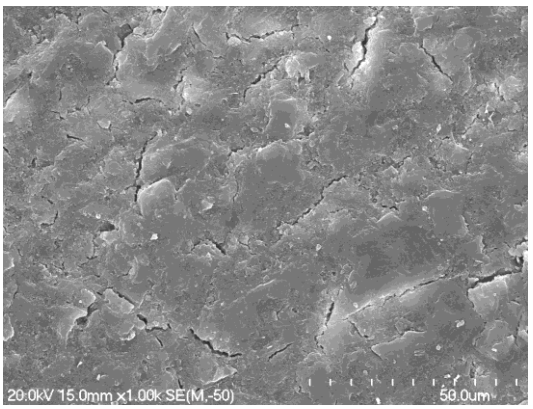

(d) Surface after etching at 1000× magnification.

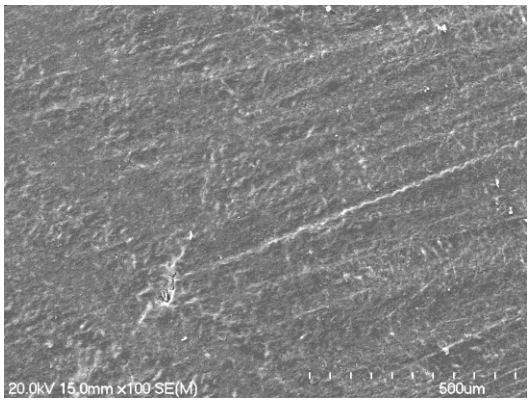

(e) Surface after sensitising.

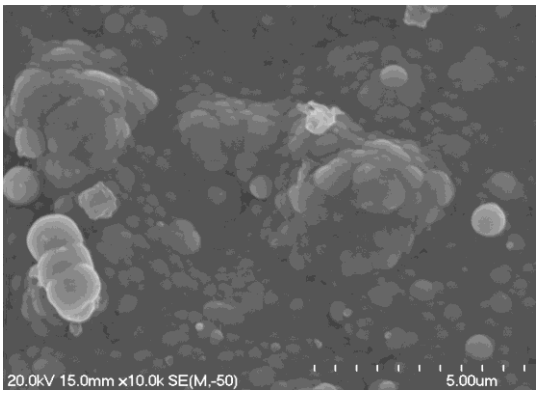

(f) Surface after electroless nickel plating.

Figure 14: The surface morphologies of the RP model during electroless nickel plating.

5.3 Elements of the Plated Surface

The energy dispersive spectroscopy (EDS) spectra for the pre-treatment processes and the electroless nickel plating process are presented in Figure 15. Figure 15(a) shows the spectra of the RP material before the pre-treatment process. Carbon (C), hydrogen (H) and oxygen (O) are the major elements of the RP material. But hydrogen is not detected due to the machine limitation. The spectrum of a nickel plated sample is presented in Figure 15(b). It shows that nickel and phosphorous are the major constituents of the layer. This is a good indication of the existence of the nickel-phosphorous alloy in the plating.

Table 5 lists the percentages of the atom counts and weight of a RP sample after nickel plating (which is extracted from the RP model as shown in Figure 12). The actual percentages of nickel and phosphorous by weight are 89% and 11% respectively after ignoring the elements of oxygen and carbon which implies a high phosphorous content in the nickel-phosphorous alloy coating.

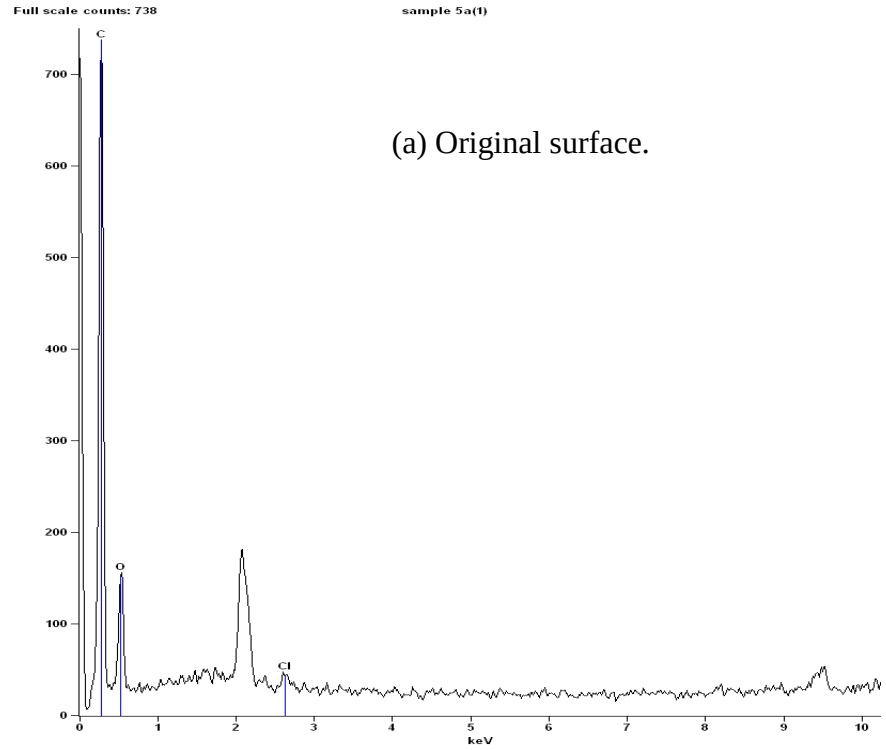

(a) Original surface.

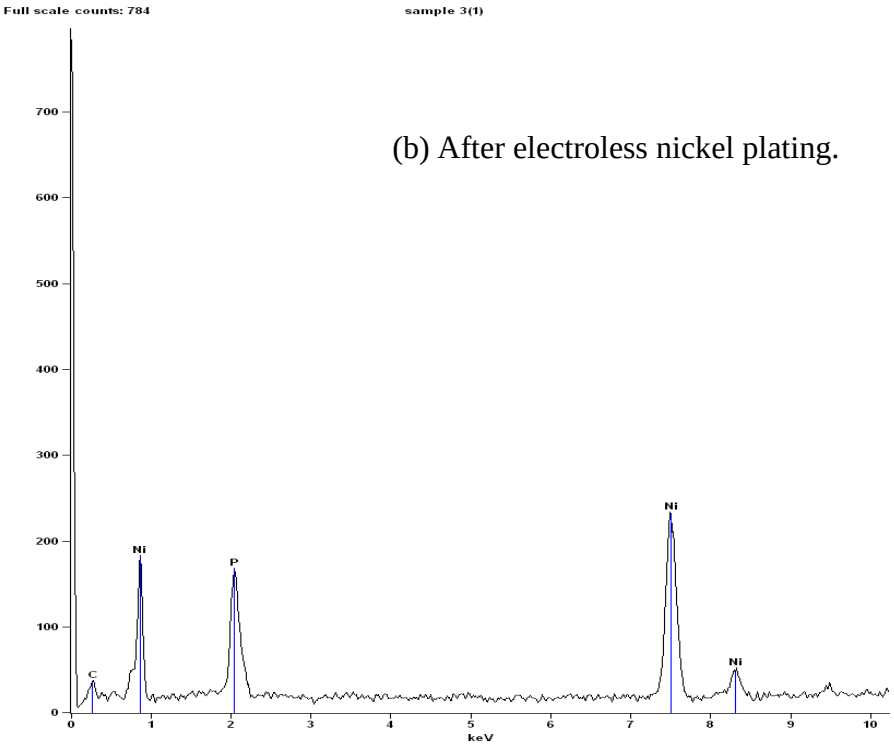

(b) After electroless nickel plating.

Figure 15: The EDS spectra of the RP model before and after nickel plating.

Table 5: EDS elemental analysis of sample from nickel plated shark model

Element	Wt%	Atom%
Ni	71.40	41.47
P	9.03	9.94
O	9.87	21.04
C	9.70	27.54

Nickel plated shark model (shown in Figure 12).

A SEM image of another RP material sample with an electroless nickel plated layer is shown in Figure 16(a) which is a cross section view. The layer thickness can be assumed as uniform without cracks or cavities between the nickel-phosphorous alloy layer and the aluminium filled epoxy resin. As shown in the figure, there is a small visible variation or one boundary is not really a straight line. This may be due to the roughness and the smearing of the outer nickel-phosphorous alloy layer when the samples are prepared. Also it can be seen that nickel-phosphorous granules are packed densely and uniformly distributed. This implies that the layer is homogenous and there are no voids and cracks development during plating. According to the EDS data as shown in Figure 16(b), the composition of the layer is mainly nickel and phosphorous after neglecting carbon. The percentage of nickel is 90% and phosphorous composition is 9.1% in this case. So according to the value 9.1% phosphorous content, the layer is high phosphorous grade electroless plating and has higher corrosion resistance than low phosphorous grade nickel – phosphorous alloy layers (Leon et al., 2010).

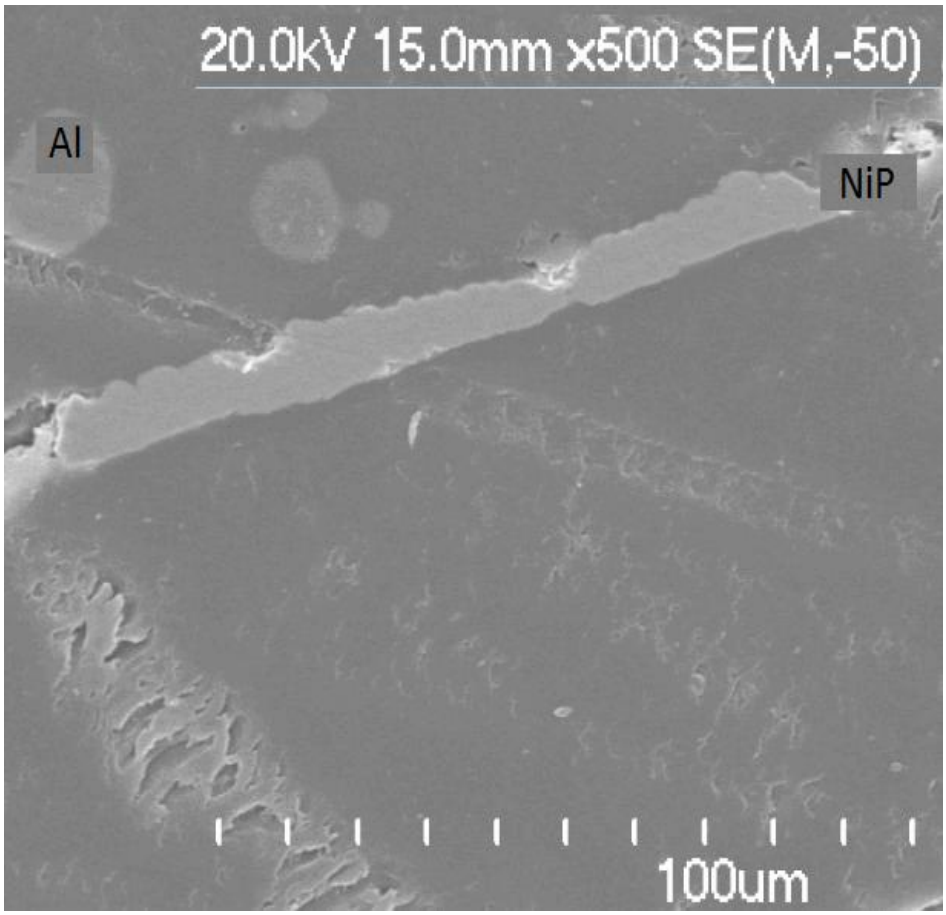

(a) SEM sectional view

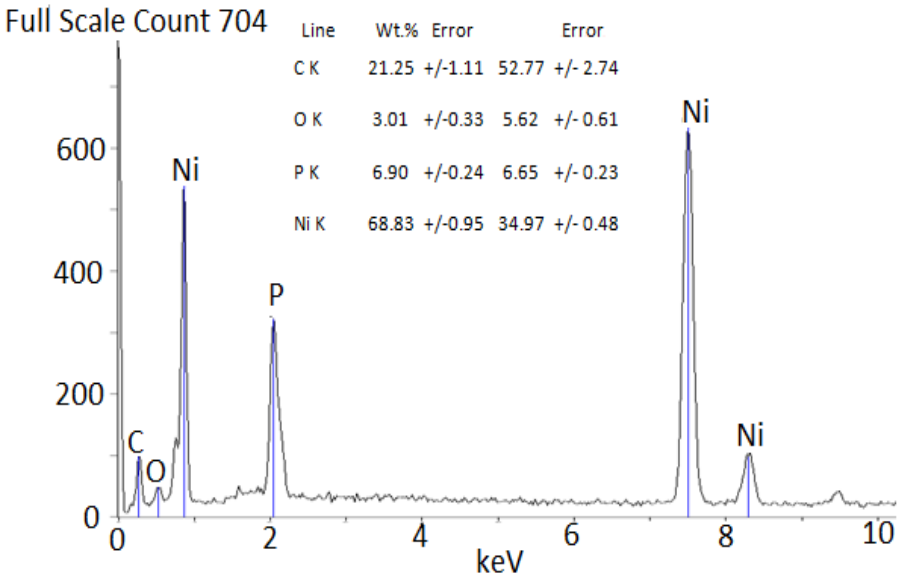

(b) EDS spectra at 5000x

Figure 16: SEM sectional view of nickel-phosphorous alloy layer and its EDS spectra

5.4 General Morphology of the Nickel-phosphorous Alloy Layer

The surface morphologies of the nickel-phosphorous alloy layer are revealed by SEM with various magnification powers.Figure 17 shows the nickel-phosphorous alloy layer with a magnification power of 60. Since the sample model is prepared by the Perfactory rapid prototyping machine with layering technique, the stair effect is still visible after the electroless nickel plating on the sample. Furthermore, the gap between the bright lines (two arrows) in the figure is measured to be 45μm which is equal to the building layer thickness of the rapid prototyping process (X/Y direction). A pre-treatment such as polishing or sand blasting of the original prototype model surface can certainly enhance the surface smoothness of the final nickel-phosphorous layer.

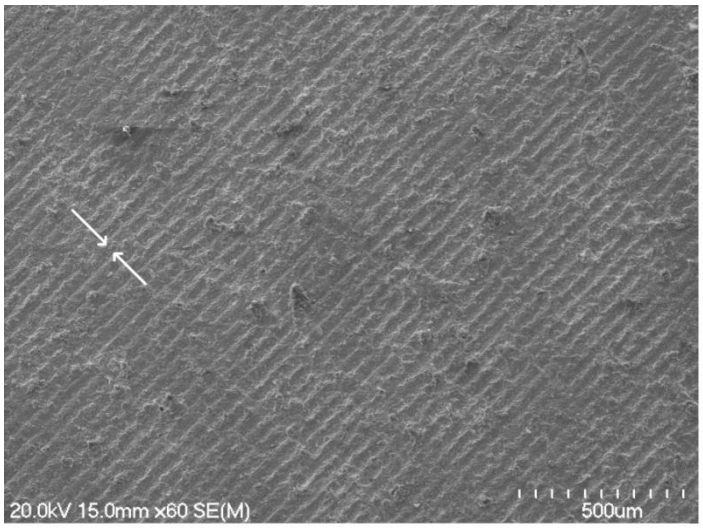

Figure 17: SEM surface image of the nickel-phosphorous alloy layer (×60).

Figure 18 presents the surface morphologies of the nickel-phosphorous alloy layer with a magnification power of 450. The spherical nodular structure of the nickel phosphorous alloy is shown in the figure and the approximate nodular diameters range from 1μm to 10 μm.

Morphology of the structure also demonstrates homogeneity and the packing uniformity of electroless nickel layer.

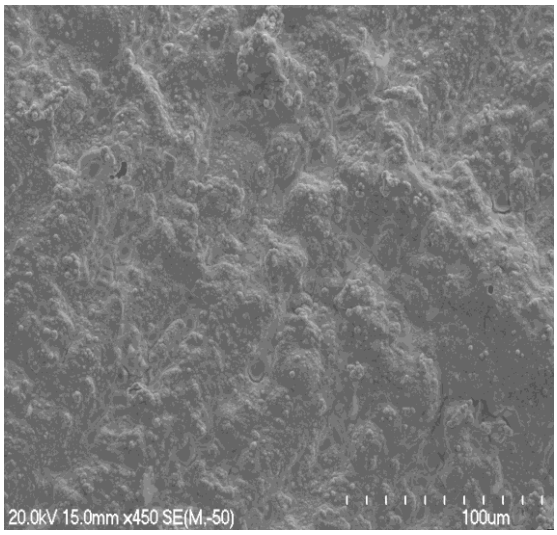

Figure 18: The SEM surface image of the nickel-phosphorous alloy layer (×450).

Figure 19 shows the SEM image with a magnification power of 800. This image is to see the difference of two materials when view through an angle. The lower part of the image shows the RP material while the cut cross section of the coating is seriously damaged with a lot of cracks and swells because of saw cut. However, there are no obvious flaws and apertures on the coating far away from the cut.

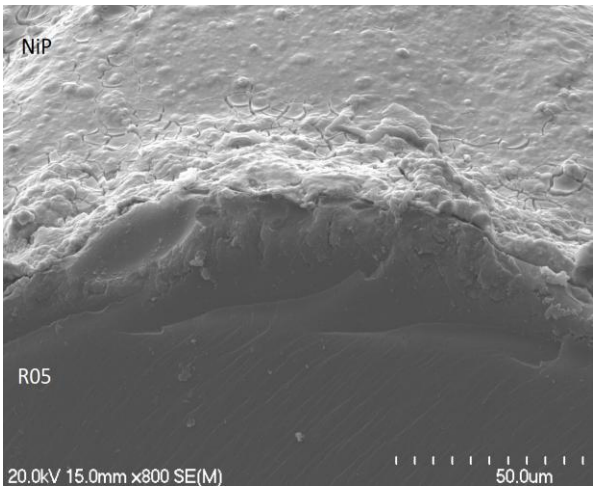

Figure 19: The SEM surface image of the nickel-phosphorous alloy layer (×800).

5.5 Micro Structure of the Nickel-phosphorous Alloy Layer

Since phosphorous has low solubility in nickel and causes lattice disorder in the crystalline nickel, the molecular structure of the nickel-phosphorous alloy largely depends upon the amount of phosphorous. If the phosphorous content exceeds 8.5% by weight, the structure of the alloy will be amorphous because of the large lattice disorder caused by the phosphorous. Crystallographic structure of the nickel-phosphorous alloy layer is studied using automatic Philips XPERT-MPD PW3373 X-ray diffraction system (XRD) with Cu K_α radiation. Figure 20 shows the X-ray diffraction pattern of nickel-phosphorous alloy (with 11% phosphorous) on the sample. Broad peaks at $2\theta = 20^o$ and 45^o in the figure suggest an amorphous structure of the nickel-phosphorous alloy coating on the sample and thus the plated layer is ductile. So it is clear that the layer structure is not pure crystal. According to the Joint Committee on Powder Diffraction Standards (JCPDS) database from the International Centre for Diffraction Data the peak representing 45^o corresponds to stable phase of nickel (JSPDS 04-0850) and that at 20^o corresponds to a meta stable phase of nickel and phosphorous i.e. Ni_5P_4 (JSPDS

18-0883). In fact, the broad peak at 45˚ becomes 111 nickel crystals (Lewis and Marshall, 1996)

This nickel-phosphorous alloy layer in amorphous state can be converted to a crystalline structure after heat treatment (Zhang et al. 2005. Liu and Gao 2006a). For instance, one hour annealing at 300˚C makes the structure crystalline and also increases its hardness. Furthermore, the coefficient of friction can also be reduced by heat treatment (Bozzini et al., 1999). The increase in the hardness is due to the precipitation of Ni_3P and increase of crystallization of the nickel-phosphorous structure (Chang et al., 2001, Wu et al., 2006).

Moreover, laser beam hardening will be a possible localised heat treatment process that can be applied on the insert to anneal the nickel-phosphorous alloy layer (Gu and Shulkin, 2000).

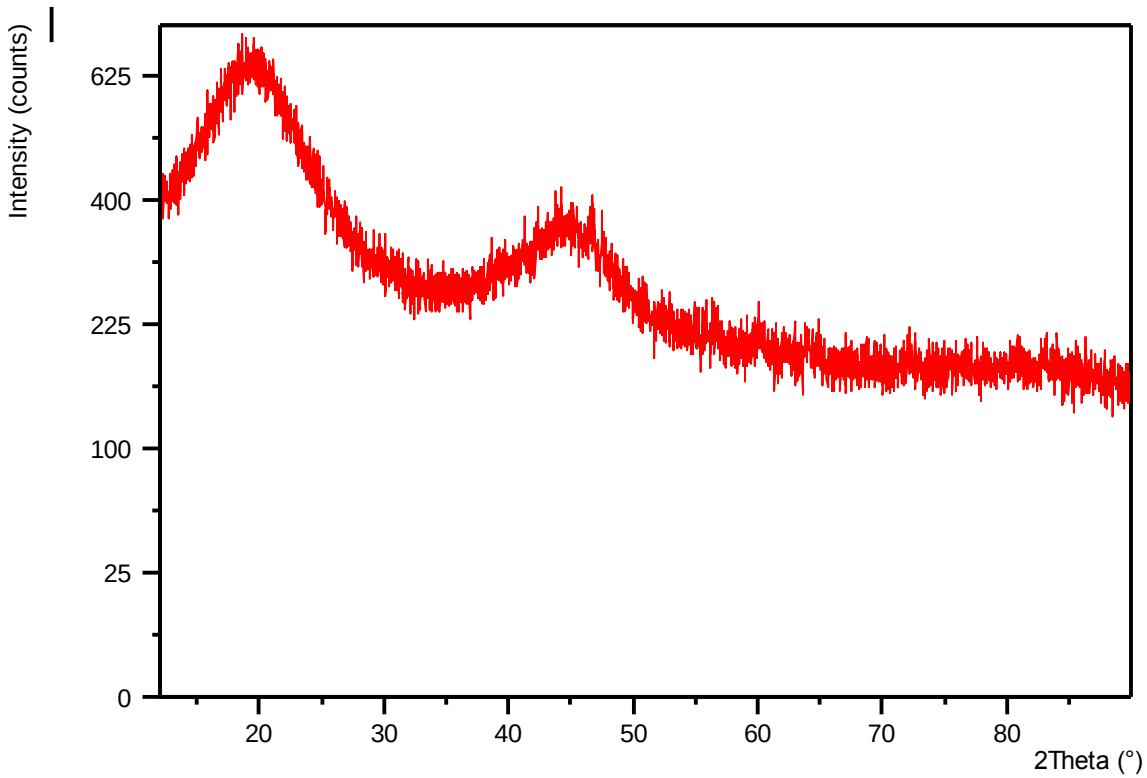

Figure 20: The XRD pattern of the nickel-phosphorous alloy on the RP system.

5.6 Nickel-phosphorous Alloy Layer Thickness Estimation

Calculation of nickel-phosphorous alloy layer thickness can be done in three ways. The first method is dependent on knowing the electroless nickel plating parameters such as chemistry, pH, bath temperature and plating time to suggest how thick the layer is. Since there are many parameters and difficulties to control them, this will lead to significant error in the estimation (Kantola and Akebom, 2010).

The second method is to examine the cross-section of nickel-phosphorous alloy layer under SEM. In order to measure thickness of the layer, a cross section of the model is fabricated by cold curing epoxy resin. The surface of the cross section is ground with silicon sand paper and polished with a rotary fabric polisher. Then an X-ray map image of the cross section is obtained by EDS. Figure 21 shows X ray map and SEM image of that cross section.

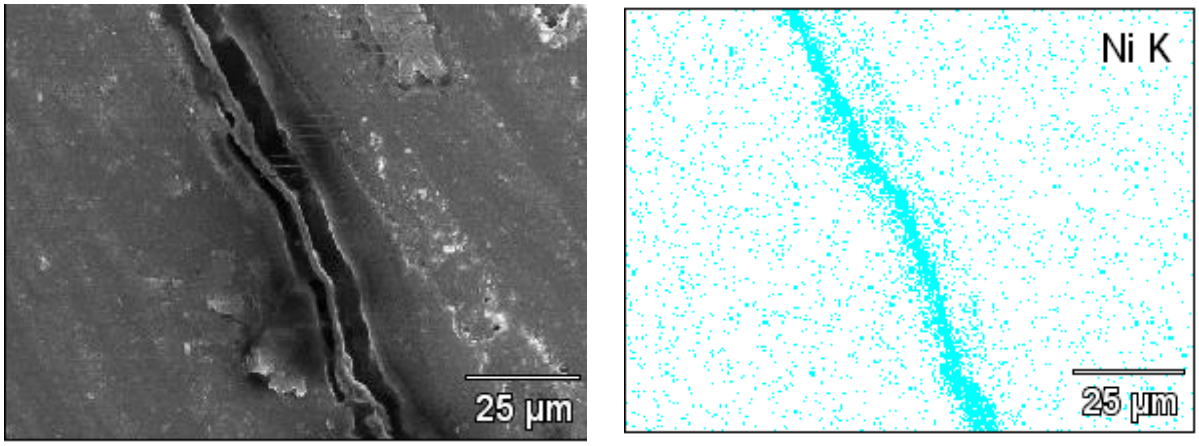

Figure 21: Section image of the layer (left) and X-ray mapping (right).

The thickness of the nickel-phosphorous alloy layer looks uniform, except that some flattening out of the edges may be due to polishing. The layer trajectory is smooth. The irregularities of the model surface replicate the same pattern of irregularities on the nickel layer. The approximate layer thickness is 2µm which is obtained by averaging the thickness measurements at several points of the SEM images. According to the X-ray mapping image, nickel is distributed uniformly over the layer with a thickness value similar to the 2µm calculated above.

Finally, the last method is to measure the layer thickness by gravity metric method. (Bulasara et al. 2011a and 2011b, Xie et al. 2011). In this method, the layer thickness is calculated from the weight gain of the substrate, density of nickel and area plated. However, errors can be introduced by the porosity of the layer.

5.7 Hardness of the Nickel-phosphorous Layer on the Cavity Insert

The surface hardness of nickel–phosphorous alloy layers is measured by using a micro hardness technique since the test is simple and non-destructive and only a small sample is required to carry out the test. In fact, it is common in practice to use a micro hardness tester for epoxy resin matrix systems (Krumova et al., 2001).

The surface hardness of the nickel–phosphorous alloy layer is measured using a Vickers micro hardness tester, Leco LM700. Data is collected from a Vickers micro hardness tester for the load range from 10gf to 1000gf for both nickel plated and the non-plated RP material using Vickers diamond indenter at 10 second dwelling time. Figure 22 tabulates the data after averaging five readings for each loading condition for both cases.

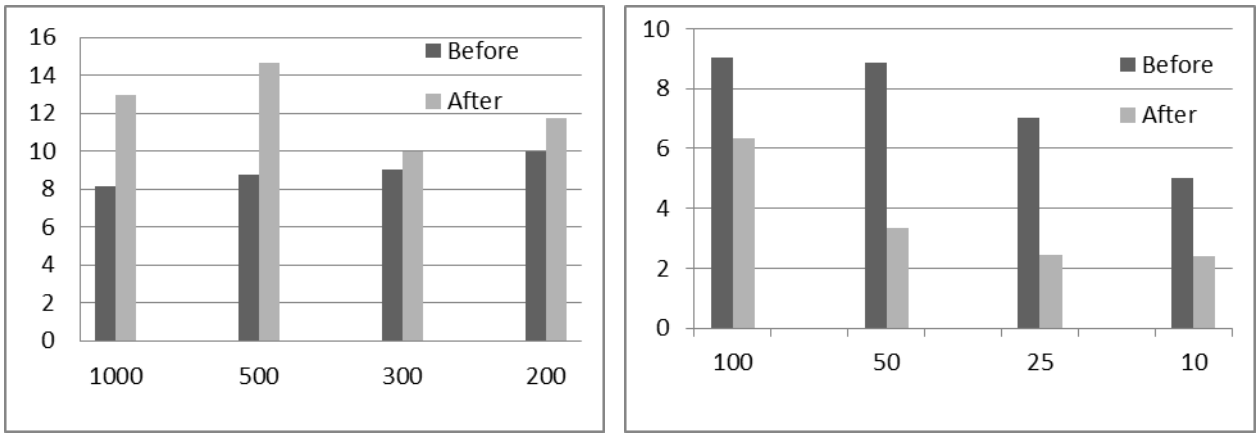

(a) loading range from 200gf to 1000gf (b) loading range from 10gf to 100gf

Figure 22: Vickers Hardness value (HV) versus loading (gf) before and after the coating.

According to the hardness data, the nickel plated surface has higher hardness value than the un-plated surface for the loading range from 1000gf to 200gf. The highest recorded Vickers hardness is $14.7HV_{500gf}$ which is 83% higher than that without plating (hardness value of $8HV_{500gf.}$).The lowest value is $10HV_{300gf}$ at 300gf loading which is 11% higher than the corresponding un-plated surface hardness value of $9HV_{300gf}$. Variation of the hardness value in this loading range is due to the local surface roughness effect. However, it is clear enough to state that the nickel plating improves the surface hardness of the RP model.

On the other hand, hardness of the plated surface exhibits a certain decrease in values in the load range from 100gf to 10gf. The largest drop is from $9HV_{50fg}$ to $3HV_{50gf}$ at 50gf loading condition which means 66% less hardness value of the coated surface than the unplanted surface. Therefore, these results show that there is no improvement in the surface hardness of the RP model with nickel plating and this contradicts the result found in 1000gf to 200gf loading range.

The contradicting result is due to the effect of surface hardness on low loading condition. For a low load on the Vickers indenter, penetration depth of the indenter can be as small as a few nanometres to a few microns depending on the material, load and indenter. Therefore, surface roughness becomes effective as less material peaks hit the tip of the indenter. So actual resistance for the indenter tip is low and the final reading is much less than the actual hardness of the material. In fact, the penetration depth of an indenter must be sufficiently deep so that the surface response to the touching indenter tip behaves according to their bulk material properties (Chung and Yap, 2005). To improve the validity of the hardness test, surface polishing can be employed which reduces the effect of surface roughness. Hardness value varies with phosphorous content (Keong et al., 2003). Here the analysis is only for one particular percentage of phosphorus present in the layer. Therefore, Vickers hardness values for low loading condition in this experiment are not reliable to use in assessing the material hardness so Vickers hardness values for high load (1000gf to 200gf) should only be considered.

Chapter 6: Plastic Injection Moulding using New RT

6.1 Introduction

The manufacturing of a cavity insert using the proposed rapid tooling approach has been presented in chapter 3. The electroless nickel plating method discussed in chapter 4 is an important process in the approach to metalize a RP model so that it can be used as a casting pattern. A cavity insert is produced by implanting the casting pattern into the bottom of the epoxy mixture with aluminium powder and taking it out after the epoxy solidification. An injection mould for low volume production is built by using the cavity insert produced by this rapid tooling technique. In this chapter, mould fabrication and injection moulding experiments will be discussed.

6.2 Injection Moulding Process Investigation

Three factors are considered in investigating the tool life of the mould built by the proposed rapid tooling approach. They are tool quality, plastic part quality and process repeatability. Among these three factors, the tool quality is the major consideration. Figure 23 shows the part to be moulded for tool life investigation. Figure 23(a) shows the RP model of the plastic part which has a nominal diameter of 20mm. Its corresponding nickel plated RP model is shown in Figure 23(b).

(a) RP model of a plastic part.

(b) Nickel plated RP model

Figure 23: Plastic part produced by the mould built by the proposed rapid tooling approach.

6.3 Cavity Insert Installation and Injection Moulding

An injection mould was built to prove the concept of this proposed rapid tooling approach. The mould was simplified by eliminating the ejection system and the water lines. The cavity insert was prepared according to the procedures presented in chapter 3 and 4 within 48 hours. It was installed in the B-plate (Moving plate) of the mould while there is no insert in the A-plate (Stationary plate) of the injection moulding machine. A pocket is prepared in the B-plate to house the cavity insert (nickel phospoprous deposited aluminium filled epoxy insert) as shown in Figure 24. The part of the injection mould is installed on the movable platen of the injection moulding machine.

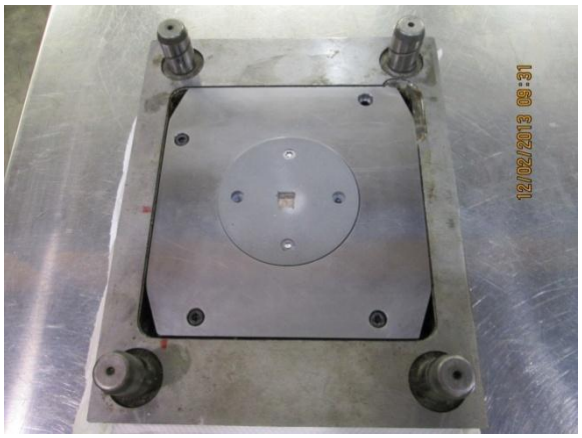

Figure 24: The cavity insert is installed in the mould base (B-plate).

An injection moulding machine BOY35A with clamping force of 350kN as shown in Figure 25 is used for the investigation. The injection moulding of plastic parts are produced continuously. The part quality and the cavity insert surfaces are observed and examined every ten shots.

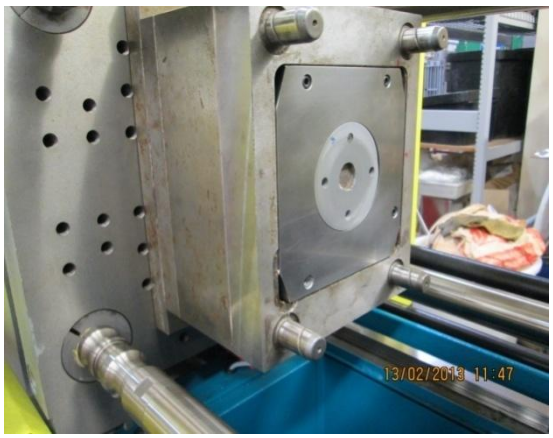

Figure 25: The mould with cavity insert manufactured by the proposed rapid tooling approach is installed on the BOY 35A injection moulding machine.

The injection moulding processing condition is listed in Table 6. Since the ejection system is not installed in the mould, silicon based mould releasing agent is used for every 100 shots.

Table 6: Injection moulding process condition

Process Condition	Value
Materials	Polyethylene
Injection Temperature	170˚C
Mould Temperature	55 ˚C
Injection Pressure	80-120bar
Injection Speed	80mm/s
Holding pressure	60-100bar
Holding time	0.1s
Cooling time	15s

The cavity insert and the casting for the investigation are shown in Figure 26. The coin is just to give an idea of the size of the finished mould.

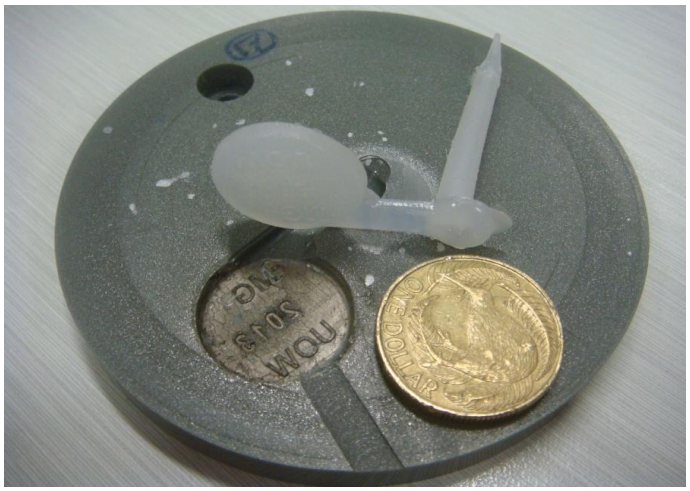

Figure 26: The cavity insert and the casting for investigation.

6.4 Part Quality

Figure 27(a) and Figure 27(b) show the plastic parts obtained by the injection mould built by the proposed rapid tooling after 107th shot and 620th shot respectively. After 620th shot, the tool does not show any deterioration in surface or delamination of the nickel-phosphorous alloy layer to the naked eye. Hence, the mould built by the proposed rapid tooling approach is capable of producing several hundred parts before surface deterioration starts. The performance is comparable to a direct metal laser sintered injection moulding insert (Nagahanumaiah and Ravi 2008). Since the nickel-phosphorous alloy layer is transferred from the plated RP model to the cavity insert during the rapid tooling process, the mould surface is getting smoother during the injection moulding trials. It is observed that flash appears along the part line after 600th shot as shown in Figure 27(b) compared to the moulding after the 107th shot as shown in Figure 27(a).

(a) Plastic part produced after 107th shot.

(b) Plastic part produced after 620th shot (flash appears along the part line).

Figure 27: Plastic part produced after 100th shot and 620th shot

6.5 Tool Quality

In order to analyse the dimension accuracy of cavity insert, feature dimensions in the RP casting pattern are compared with the same feature's dimension in the cavity insert. Three features namely "G", "O" and "1" on the both casting pattern and the cavity insert are observed through an optical microscope. The thickness of the symbols are measured and listed in Table 7.

Table 7: Dimensional comparison of the casting pattern with the cavity insert

Feature	Casting pattern (µm)	Cavity insert (µm)	Percentage difference (%)
"G"	365	360	1.3
"O"	365	360	1.3
"1"	300	290	3.3

According to the optical microscope measurements of the selected features on the casting pattern and the cavity insert, the difference in the thickness of “G” and “O” is only 1.3% which is considered to be acceptable so that the process is able to produce features with good accuracy. The Feature “1” produces 3.3% difference which is higher than the measurements of the other two features. The reason could be the shrinkage of the aluminium filled epoxy insert, thickness of nickel-phosphorous alloy layer and estimation errors from the optical microscope.

The most obvious phenomenon to determine the tool life is to investigate the quality and surface properties of the cavity insert. Such investigations are performed at the start of 107th, 320th, 620th shot respectively. According to the visual inspection there is no obvious surface defect on the cavity insert. Figure 28(a) and Figure 28(b) show the cavity insert surfaces after the 107th shot and the 620th shot respectively.

(a) After the 107th shot

(b) After the 620th shot

Figure 28: Cavity insert surface after 107th and 620th shot.

Basically, there is no wear on the nickel-phosphorous alloy layer except for the very little peel off after 620th shot in the vertical edge of the cavity insert. However, there is still no further abrasion wear on the aluminium filled epoxy resin after peeling off the nickel-phosphorous alloy layer. As the thickness of the nickel-phosphorous alloy layer is just a few microns, it does not cause any visual defects on the surface of the plastic part.

Figure 29 shows the magnified optical microscope images of the cavity insert on a selected feature letter "G" at the beginning, after the 107th shot, after the 320th shot and after the 620th shot respectively. The optical microscope images of relevant part of the cavity insert at about 5× magnification also do not show any significant variation or changes of surface quality, dimensional accuracy or roughness. This implies that the cavity insert has good performance during the injection moulding cycles. Hence, the cavity insert can be used to produce injection moulded plastic parts for low and intermediate production volume. The performance can be varied with the polymer resin and processing parameters such as injection pressure and temperature. For the polyethylene used in this investigation the process works well.

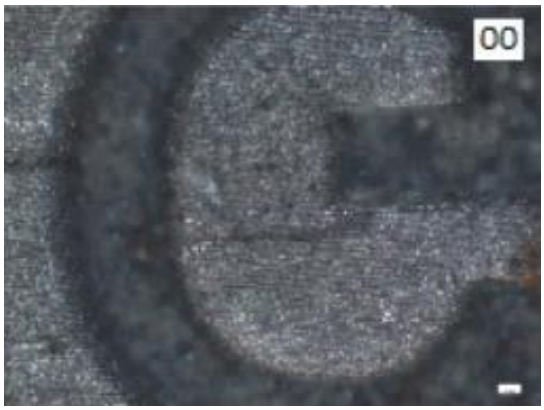

(a) At the beginning of the investigation.

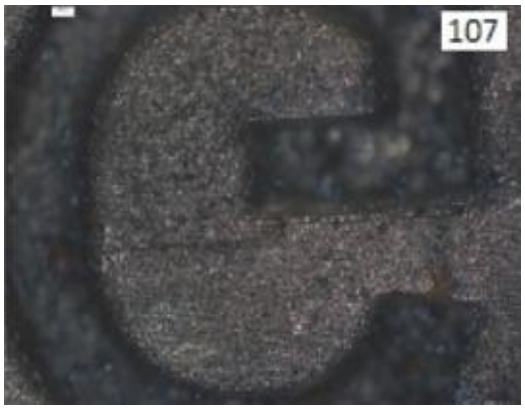

(b) After the 107th shot.

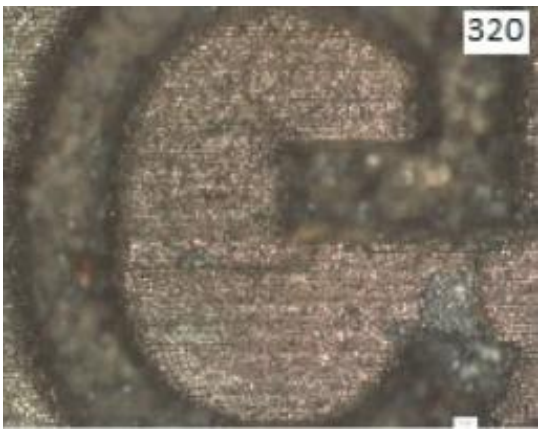

(c) After the 320th shot.

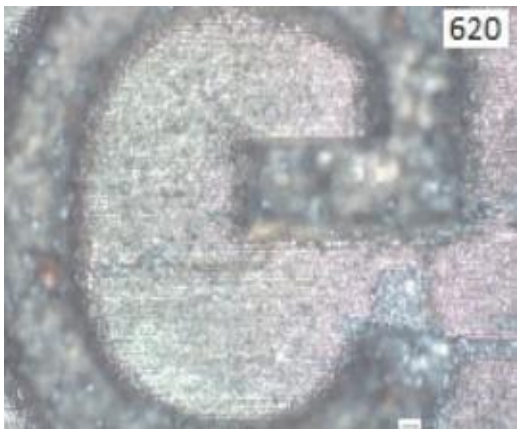

(d) After the 620th shot.

Figure 29: The magnified optical microscope images of the cavity insert surface.

The optical microscope images of letter “G” of the casting pattern and cavity insert are shown in Figure 30. It is clear that both surface textures and roughness are similar. The surface texture of the cavity insert at the letter “G” is replicated almost the same as that of the casting pattern. The stair effect of Perfactory building technique is also visible in the optical microscope images (which should be invisible to naked eye). There is no evidence of cracks in the nickel-phosphorous alloy layer. However, there is a damaged portion in the cavity insert. It may have been damaged when detaching the casting pattern which can be avoided by doing it carefully.

(a) Perfactory RP model (b) Cavity insert

Figure 30: Comparison of the surface on the RP model and the cavity insert.

Besides the number of shots, the effect of injection pressure to the cavity insert is also examined. Some cracks initiated at the sharp edges as injection pressure increases beyond 120 bar. Catastrophic failure of the cavity insert due to crack propagation is influenced by loss of storage modulus. This is because of the temperature rise in the cavity insert material during the filling stage. In fact, nano scale filler can be used in the epoxy to improve the ductility and opacity (Zhao et al. 2008).

Thermographic images of both cavity insert and casting as shown in Figure 31 were taken using an infra-red camera, FLIR ThermaCam P640. It is factory calibarated to best possible thermal images and recalibration is done annually. The pictures are taken at about 40s after the injection. The hottest part of the mould is about 71.5˚C as shown in Figure 31(a) and that of cavity insert is about 53.5 ˚C as shown in Figure 31(b).

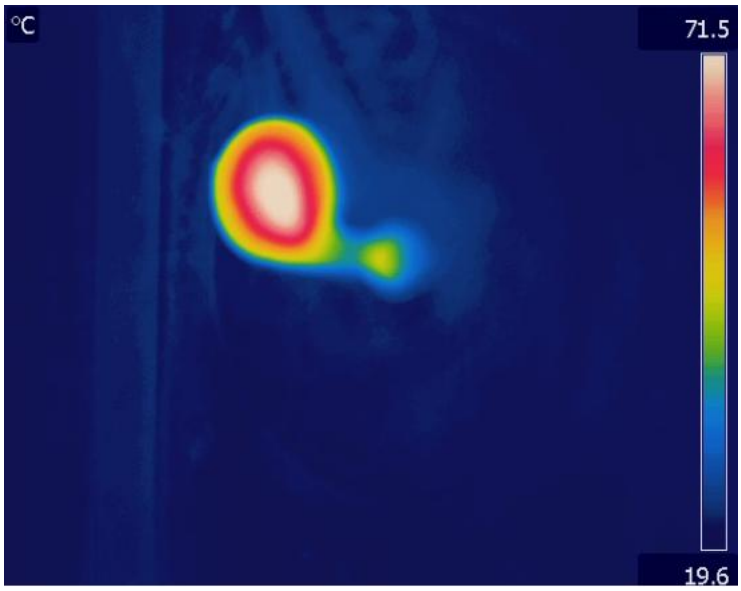

(a) The mould temperature

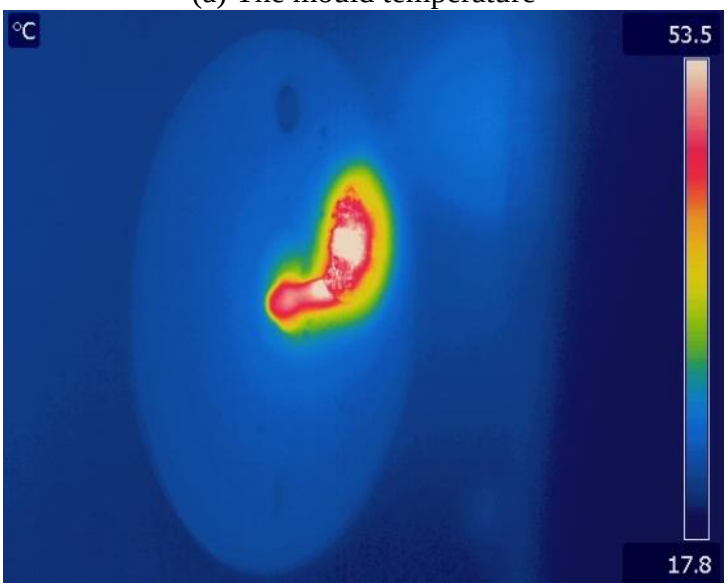

(b) The casting temperature

Figure 31: The thermographic images of the cavity insert and the casting.

This information is useful since the cavity insert temperature is well below glass transition temperature of the epoxy resin when the mould is just opened. This cycle temperature is better than the cycle temperature obtained for Stereolithography inserts reported elsewhere. The

cavity insert gains its strength for the next injection moulding shot in a short time. This property of lower mould temperature is due to the addition of aluminium particles. Thus, the production can be run at a faster moulding cycle for high productivity which is 45s in this investigation.

Although there is no ejection system installed in the mould, failure in manual ejection has not been observed in this investigation. In fact, high aspect ratio features are prone to ejection failure (Palmer and Colton, 2000). Furthermore, the ejection force required to de-mould the part also relies on the hardness of the cavity insert material. The aluminium filled epoxy resin is cured at room temperature for 24 hours when it is prepared, but the manufacturer data suggests that even after 24 hours, the material can still undergo polymerization (West System, 2010). Therefore, as the number of shots increases, the aluminium filled epoxy resin in the cavity insert further cures and becomes harder which reduces the ejection force to knock out the casting.

6.6 Process Repeatability

Different parts of similar dimension were used to investigate the process repeatability of a mould built by the rapid tooling approach. A square plastic part with nominal dimension 20mm×20mm×2mm was moulded by the process conditions listed in Table 8.

Table 8: Injection moulding process condition for the square part

Process Condition	Value
Materials	Polyethylene
Injection Temperature	170˚C
Mould Temperature	55 ˚C
Injection Pressure	85bar
Injection Speed	85mm/s
Holding pressure	90bar
Holding time	0.1s
Cooling time	16s

The square part and the mould after 650th shot are show in Figure 32.

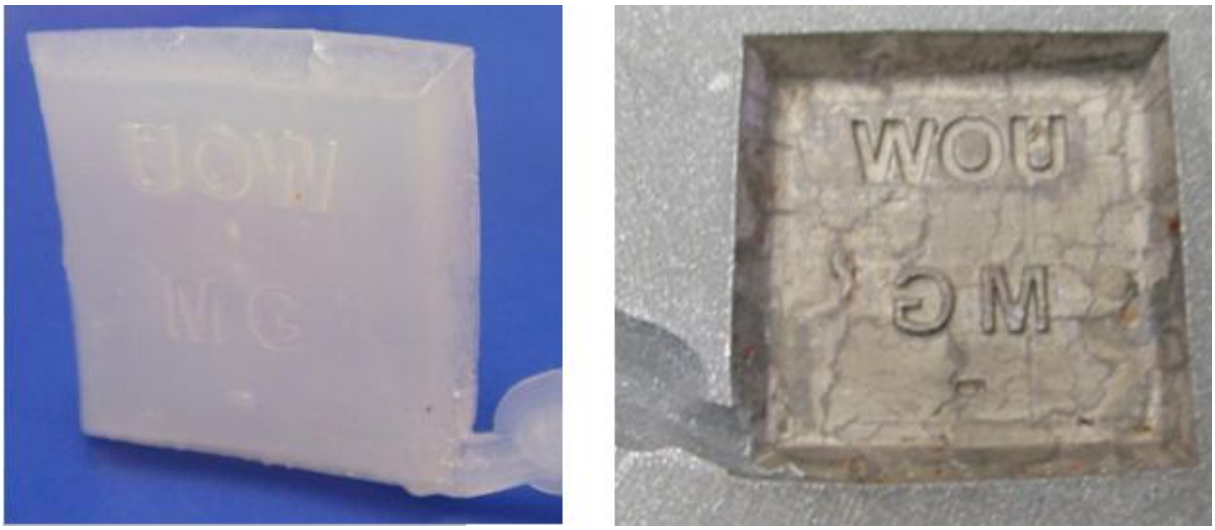

(a) Square part at 650th shot (b) Cavity insert after 650th shot

Figure 32: A square part produced by the mould built by new method.

The other trapezium part of nominal dimension 35mm×25mm×5m is also moulded with the process conditions listed in Table 9 for process repeatability investigation.

Table 9: Injection moulding process condition for the trapezium part

Process Condition	Value
Materials	Polyethylene
Injection Temperature	170˚C
Mould Temperature	55 ˚C
Injection Pressure	110bar
Injection Speed	105mm/s
Holding pressure	105bar
Holding time	0.3s
Cooling time	30s

The trapezium part and the mould after 650th shot are shown in Figure 33

(a) Trapezium part at the 650th shot. (b) Cavity insert after 650th shot

Figure 33: A trapezium part produced by the mould built by rapid tooling.

Both injection moulds were built within 36 hours. The nominal dimensions of these after 650^{th} shot for both parts do not show any significant variations. In fact, the sizes are quite consistent for this low volume production. It can be seen from Figure 32(a) and Figure 33(a) that both parts at the 650^{th} shot do not have any obvious surface defects. Since the simple injection mould is not equipped with water lines, warping exists due to the uneven cooling effect. The dimensional accuracy between the RP model and the moulded parts in both cases are within 5% difference.

However, the cracks appear on the nickel-phosphorous alloy layer of the cavity insert for the square part as shown in Figure 32(b) .On the other hand, the nickel-phosphorous alloy layer on the cavity insert for the trapezium part starts peeling off although it does not affect the plastic part as the layer is thin.

Chapter 7: Discussion

7.1 Introduction

This chapter discusses various properties of the aluminium filled epoxy resin as it is the major material in the cavity insert. The properties of this material contribute to the tool life which affects the plastic part production volume.

A Perfactory RP machine is capable of producing fine features. The smallest feature in this research is about 400μm and it is a usual feature size for many consumer products. The Perfactory model has good surface finishing. Plating a uniform layer of nickel-phosphorous alloy layer on the RP model does not de-feature the part as the plating layer is thin.

7.2 Aluminium Filled Epoxy Resin Preparation

Epoxy resin is a popular material for building injection moulds for low volume production. It is also common to fill with reinforced materials to improve the mechanical and thermal properties. However the intrinsic brittleness of the material hinders it application in structures (Kim et al., 2003).

Various metal powder particles are used as filler elements for epoxy resin systems in practice. In this research, the commonly available and economical aluminium particles are used. Actually, the same powder is also used as filler for reinforcement in different engineering applications. Addition of aluminium power not only improves wear of the cavity insert, it also improves the thermal conductivity capacity (Vasconcelos et al., 2005) and surface hardness of

the material (Vojdani et al., 2012). These attributes are exploited in this research since high pressure and resin temperature are common processing conditions in injection moulding.

The aluminium powder was provided by Sigma Alrich and is used as received. The particle size is about 45μm normally spherical in shape. This fine size and low aspect ratio filler enhances the impact resistance of the mixture once cured (Perkins, 1999). Some of the important properties of cured epoxy resin can be found from West System, 2010

Mixing the epoxy system with an extra 10% of aluminium powder increases the thermal conductivity by over 200% (Kilik et al. 1989b) whereas the increase of thermal conductivity is even higher if silver powder is used (Bjorneklett et al., 1992). Actually, different percentages of aluminium powder are used for various applications. Moreover, the epoxy adhesive can also be modified by the polymer and metal powder proportion which improves the teratology and surface energy (Brostow et al. 2010). Other characteristics such as electric conductivity, paramagnetic, mechanical and thermal properties can also be enhanced.

In this research, an extra 10% of aluminium powder is used to build the cavity insert to raise the thermal conductivity. The aluminium is micro powder and no polymer is used to modify the resin mixture other than the curing agent suggested by the vendor. The curing rate is low (which takes 24 hours) but it does not affect the speed of the proposed rapid tooling approach as the epoxy can be cured overnight. The epoxy is ready on the next day afternoon for taking out the casting pattern and installing onto the mould base.

Epoxy resin is an adhesive resin with high adhesive strength and high heat resistance (Sugihara et al. 1996). Foam always forms during the epoxy resin preparation. This may be due to the vapour of condensed water, ammonia and formaldehyde as the curing proceeds. These bubbles affect the mechanical properties of the cavity insert. In this research, the

casting pattern is implanted at the bottom of the aluminium filled epoxy resin. The foam generated during curing will rise up to the top surface and release to the atmosphere. Even the air entrapped in the aluminium filled epoxy resin has sufficient time to rise upward and escape to the atmosphere so that the nickel-phosphorous alloy layer outside the casting pattern is surrounded by the homogeneous epoxy resin.

Internal stress is another issue in epoxy tooling due to cooling down from curing temperature to service temperature. These internal stresses have strong influence on the mechanical properties of the composite materials and depend on the cure process, filler type, filler shape, filler content and dispersion (Goyanes et al., 2003). But the curing of the proposed rapid tooling approach takes place at room temperature so that there is no heat gain or loss to build up the stress. Hence, the internal stress built up in the epoxy can be considered to be limited due to the small temperature rise during polymerization.

Finally, various fillers such as glass fibre, carbon fibre, rubber and silica can added to epoxy resin to improve the tribological properties of the composite for various applications such as rapid tooling (Vasconcelos et al. 2006). However, no other filler is used in this research and the cavity insert (with the nickel-phosphorous alloy layer transferred from the casting pattern) lends good tribological properties.

7.3 Mechanical Properties of Aluminium Filled Epoxy Resin

The flexural property of the aluminium filled epoxy resin samples (40mm span) was measured by using an Instron universal tensile testing machine with cross head speed of 0.5m/min and 5kN load cell. The variation of flexural strength and tensile strength versus

aluminium content is given in Table 10. Three samples were tested per one aluminium content and worked out the average value.

Table 10: Tensile and flexural strength with and without nickel-phosphorous alloy layer

Aluminium content (%)	Tensile Strength (MPa)	Flexural Strength (MPa)
10%	38.2	83.1
30%	34.2	59.7
50%	33.6	65.4

The tensile strength decreases as the percentage of aluminium content increases. This may be due to the poor bonding between the aluminium and epoxy resin, especially when air is trapped in the epoxy composite (Karalekas 2003b, Karalekas and, Ntoniou, 2004) as the applied stress does not transfer through the interface when the bonding is poor (Hassan et al., 2011). Hence, the material behaves more like a brittle material and because of this it was difficult to obtain the tensile strength at the failure when the content of aluminium particles was high. It can therefore be concluded that the introduction of aluminium particles into the epoxy resin induces brittleness. The crack initiation and propagation from the Vickers micro indentation marks provide evidence of the loss of tensile strength of the aluminium filled epoxy resin samples. The variation of flexural strength could not be explained.

7.4 Surface Preparation of Nickel-phosphorous Alloy Layer

The factors governing the adhesion of the aluminium filled epoxy resin to the nickel-phosphorous layer are mechanical inter locking, chemical bonding and surface energies (Derek, 2009). In this case, the higher surface roughness of the aluminium filled epoxy resin side certainly increases mechanical inter locking. Also it can be controlled by chemical concentration, plating time and temperature of plating (Furukawa and Mehregany, 1996). Furthermore, there should be chemical covalent bonding between nickel and aluminium filled epoxy resin. Figure 34 shows the distribution of nickel and phosphorous in the alloy layer by using EDS X – Ray mapping. It can be seen that nickel is distributed uniformly over the surface; therefore the adhesion due to chemical and mechanical interlocking should be uniform as well.

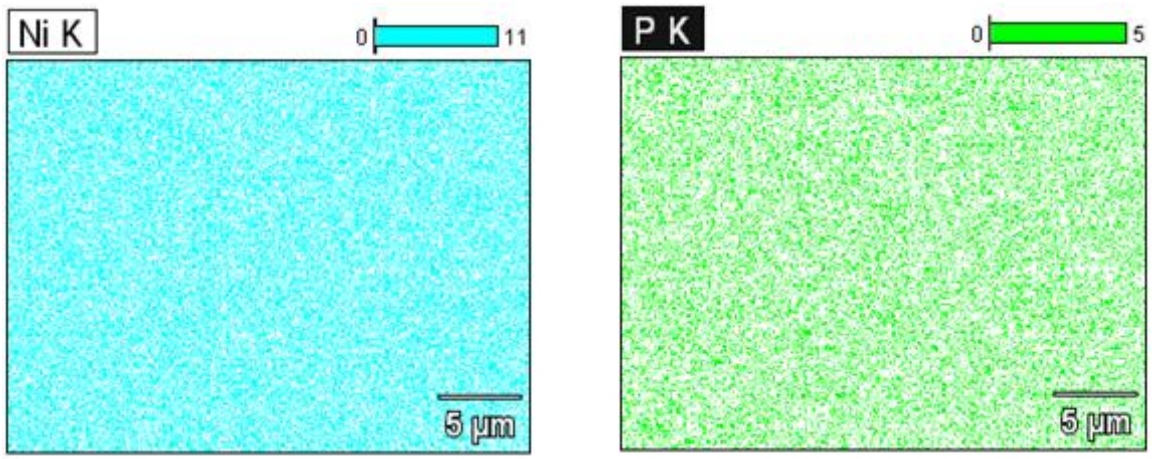

Figure 34: EDS X – Ray mapping of nickel-phosphorous alloy layer

Figure 35 shows the morphology of the first nickel-phosphorous alloy layer plated to RP material and the last nickel-phosphorous alloy layer adhere to the aluminium filled epoxy

resin of the cavity insert. In both morphologies, the nickel-phosphorous alloy granule sizes are similar. They are densely packed and uniformly distributed.

There is a small area where loss of nickel-phosphorous alloy elements is visible. That is probably due to the peeling of a small portion of the nickel-phosphorous alloy layer when the casting pattern is removed. The sizes of nodules that make up the surface roughness are around 1-3μm (Wu et al. 2003 and Balaraju et al. 2007a). The size of grains is small for high phosphorous content and transition to amorphous structure (Lu and Zangari, 2002). The globular particles are densely packed thus it can be assumed that the nickel-phosphorous alloy layer has no porosity (Roy and Sahoo, 2010). However, the nickel-phosphorous alloy deposits can form pores, precipices, segregation and micro cracks because of dehydrogenation during the catalytic process (Lin et al., 1997). According to the morphology, the pores in grains or grain boundaries are not visible to naked eye.

In the both surfaces, there is a noticeable roughness and no obvious flaws or apertures. The peaks and valley nature of second surface are significant. Therefore, surface roughness of the first layer should be same as the surface roughness of the casting pattern. So the nickel-phosphorous alloy layer is able to duplicate the RP casting pattern surface roughness to the aluminium filled epoxy resin cavity insert. On the other hand, in the casting pattern side of the first layer, the peaks and valleys are flat compared to the aluminium filled epoxy resin side of the second surface. That means that the surface exposed to curing aluminium filled epoxy resin has a high roughness and providing a higher adhesive level to the epoxy resin side than adhesion to the casting pattern. This roughness can be further increased by incorporating a third element such as alpha alumina particles (Alirezaei et al., 2007). So the outer surface with high mechanical roughness after plating is an effective factor to enhance the adhesion of

epoxy Griffiths et al. (2007). In fact, the tool surface roughness has an influence on part quality and melt flow. A smooth surface experiences less shear rate and slip stick effect.

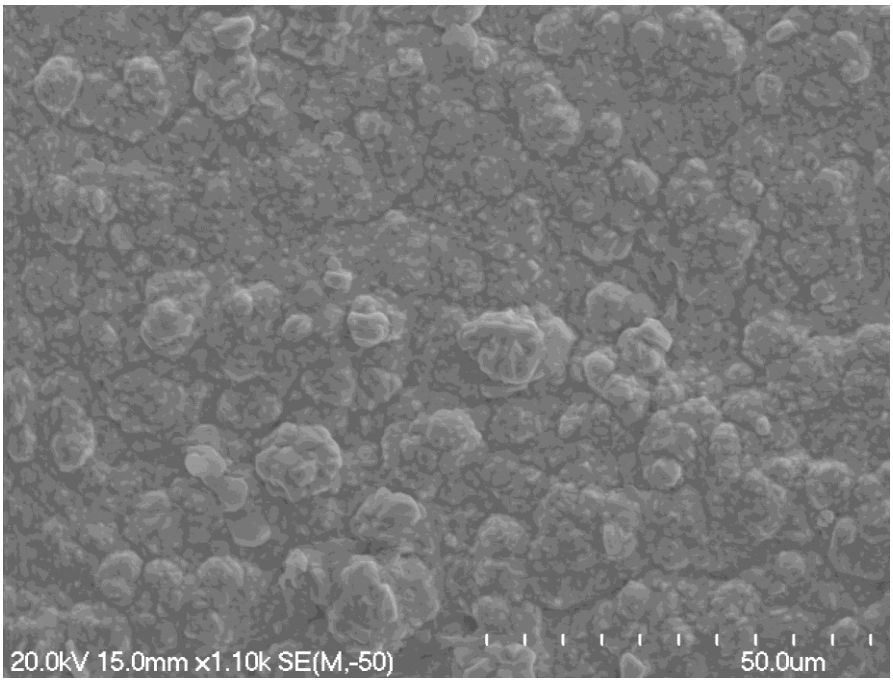

(a) The first layer

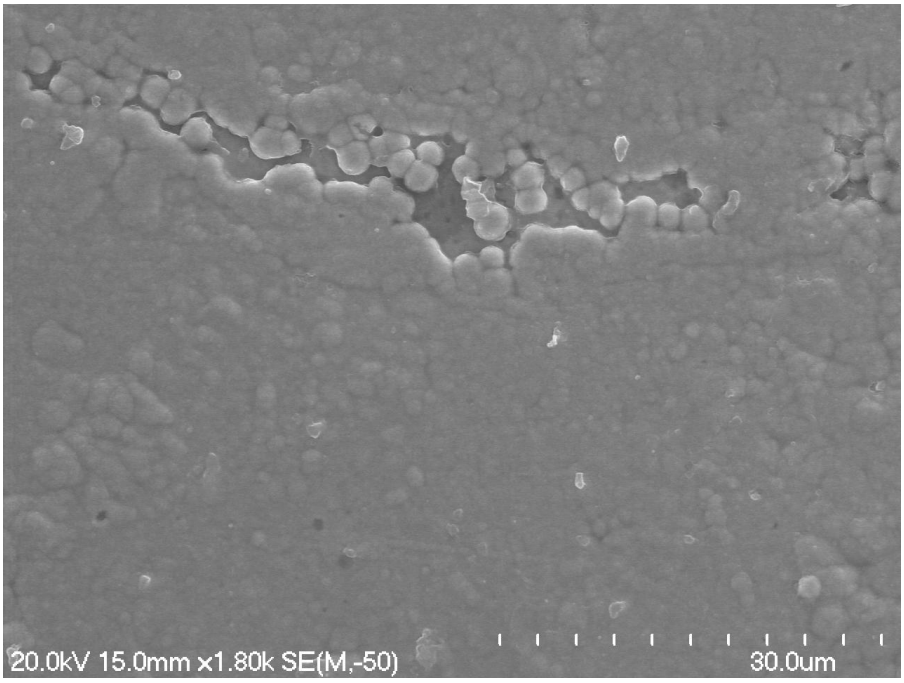

(b) The last layer

Figure 35: Morphology of nickel-phosphorous alloy layer

7.5 Hardness of Aluminium Filled Epoxy Resin

Since the Prefatory R5 RP material is a soft material, a layer of nickel-phosphorous alloy is coated on the outer surfaces of the casting pattern before it is implanted in the epoxy. After the removal of the casting pattern, the nickel-phosphorous alloy layer will be left on the epoxy cavity insert. This actually forms a layer of protection to the mould cavity. The nickel-phosphorous alloy layer plated on the casting pattern should not be exposed to air for a long time since this leads to the increasing possibility of forming nickel oxides (NiO, Ni_2O_3). This will seriously reduce the direct adhesion between epoxy and the nickel-phosphorous alloy layer (Mori et al., 1997).

A hardness test was carried out on the aluminium filled epoxy resin with and without the nickel-phosphorous alloy layer. According to the hardness data listed in Table 11, the epoxy sample with a nickel-phosphorous alloy layer has a higher hardness value than the epoxy sample without nickel-phosphorous alloy layer for loading range from 10gf to 1000gf. Five readings were taken per one loading condition and the average value was calculated.

Table 11: Micro Vickers Hardness (MHV) testing of aluminium filled epoxy with and without nickel-phosphorous alloy layer.

Indenter load (gf)	Aluminium filled epoxy (MHV)	Aluminium filled epoxy with nickel-phosphorous alloy layer (MHV)
0010	09.8	25.8
0025	12.6	23.6
0050	13.7	21.4
0200	13.8	20.4
0500	14.1	20.1
1000	14.5	17.8

The highest recorded Vickers hardness value for the epoxy sample with nickel-phosphorous alloy layer is 25.8HV_{10gf}. This is 163% higher than that of sample without the alloy layer which is only 9.8MHV_{10gf}. For the nickel-phosphorous alloy layer, hardness values are inversely proportional to the indenter load. The highest hardness value of the plated sample is 25.8 MHV_{10gf} and the lowest is 17.8 MHV_{10gf}. The factors effecting such a variation are the indenter penetration depth and surface roughness effect (Wai et al., 2004). At high loads, the value is more likely to match the bulk aluminium filled epoxy resin properties as the penetration depth is deeper than the nickel-phosphorous layer (Chung and Yup, 2005). But at low loads such as 10gf, the hardness values are attributes of the properties of the nickel-phosphorous alloy layer. Therefore, hardness values at low load conditions yield better hardness estimations than high loads.

Furthermore, the variation of hardness for aluminium filled epoxy resin shows an opposite trend. The indenter loading is directly proportional to the micro hardness value. This opposite trend is due to the effect of embedded aluminium particles. At high load, the indentation is deeper. Thus the indenter has to break and resist not only epoxy resin but also a significant amount of aluminium particles. Since aluminium is harder than cured epoxy resin, so the hardness is higher at high load. At low loads i.e. 10gf, the indenter is aligned to hit only epoxy resin, so the hard aluminium particles have no effect on the low hardness value. In fact this value represents the hardness of cured epoxy resin only. In conclusion, according to Table 11, a nickel-phosphorous alloy layer improves the surface hardness of the cavity insert and so does the aluminium particles (Chung and Yap, 2005 and Qin et al., 2010).

7.6 Thermal Behaviour of Aluminium Filled Epoxy Resin

Thermal properties of the photopolymer materials are very different to either a steel or aluminium mould. Understanding the thermal properties is important since it has influence on injection moulding cycles and the final properties of the casting parts (Kovacs et al., 2011). The temperature dependent mechanical quality of the epoxy is measured by a dynamic thermal mechanical analyser (Deng et al., 2007). Rectangular samples of aluminium filled epoxy resin (2mmX5mmX20mm) are subjected to single cantilever bending test using Perkin Elmer Dynamic Thermal Mechanical Analyser, DMA8000 at a heating rate of 5 ˚C per min at 1Hz from room temperature to 150 ˚C under normal atmospheric pressure. The beam displacement is set to 50µm

According to Figure 36, the storage modulus starts to drop after around 50˚C. The glass transition temperatures are improved a little with the addition of aluminium powder and further improved by the nickel-phosphorous alloy layer.

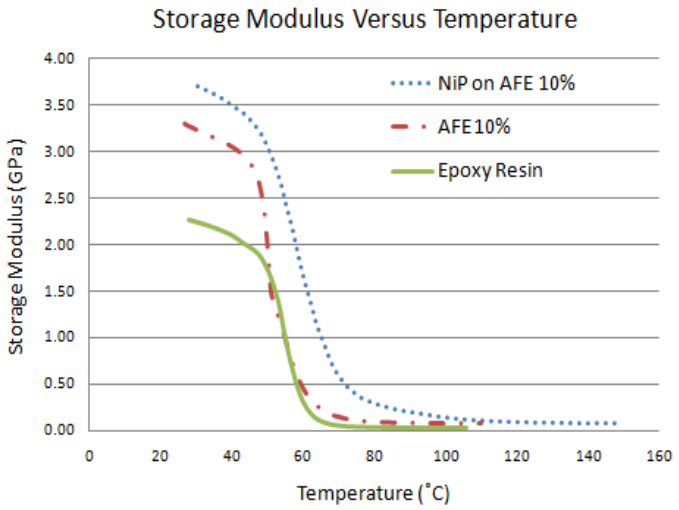

Figure 36: Storage modulus of aluminium filled epoxy resin versus temperature

The highest storage modulus is observed when the sample is plated with nickel-phosphorous alloy layer. Neat cured epoxy represents the lowest storage modulus. Further that graph shows that as the epoxy matrix materials get reinforced, it becomes resistive to the temperature (higher storage modulus) lending better mechanical properties. Furthermore, the nickel-phosphorous alloy layer improves the thermal properties of the cavity insert, as the storage modulus of aluminium filled epoxy resin with nickel-phosphorous alloy layer drops to nearly zero after about 120˚C, whereas it is about 70˚C for neat epoxy resin. Therefore, nickel-phosphorous alloy plated aluminium filled epoxy resin gives better thermal properties which is good for applications like injection moulding and casting.

Figure 37 shows the variation of tanδ (Ratio of storage modulus to loss modulus) with temperature for three samples: epoxy resin, aluminium filled epoxy resin and aluminium filled epoxy resin plated with nickel-phosphorous layer. Based on the maximum tan δ value, the glass transition temperature of both epoxy resin and aluminium filled epoxy resin are about 50˚C. The aluminium filled epoxy resin with nickel-phosphorous layer has a higher glass transition temperature of almost 75˚C.

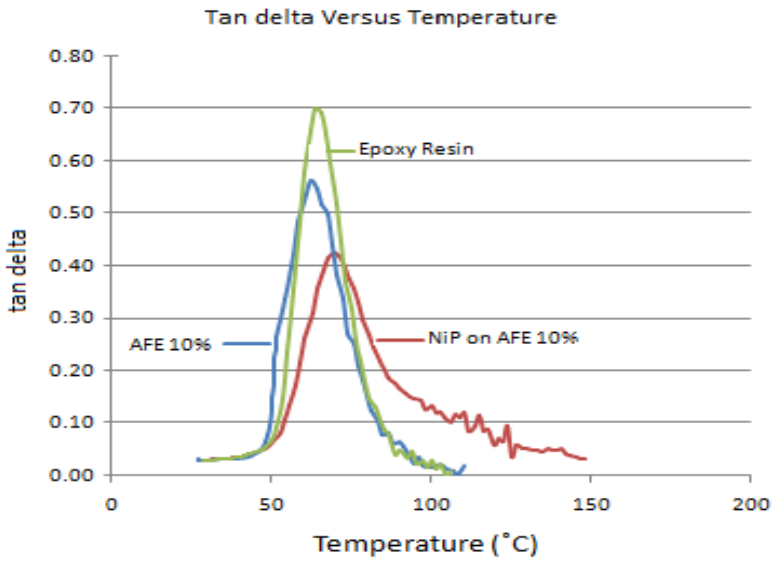

Figure 37: tan δ of aluminium filled epoxy resin versus temperature

7.7 Adhesive of Nickel-phosphorous Alloy Layer on Aluminium Filled Epoxy Resin

Adhesion is an important parameter in this research because it can be attributed to the bond strength between these two dissimilar materials namely nickel-phosphorous layer and aluminium filled epoxy resin.

The surface free energy of the nickel-phosphorous layer gives a direct measure of intermolecular interaction at interfaces and has a strong influence on wetting, absorption and adhesion (Zhao et al., 2005 and Zhao et al., 2000). The nickel-phosphorous micro structure also has some influence on its surface free energy (Cheng et al. 2009).An amorphous matrix has a low surface free energy whereas a crystalline deposition has higher surface free energy.

However the force or interaction between epoxy resin and nickel-phosphorous can be high. The interfacial mechanical interlocking effect plays a more important role in improving adhesion strength and substrate composition and micro structure leads to different surface roughness. Therefore, the nickel-phosphorous and aluminium filled epoxy are bonded strongly by mechanical interlocking and chemical bonds (Liu and Gao 2006b).In fact, the interface ascribes to many processes like segregation, selective absorption, hindrance and curing shrinkage (Possart et al. 2009).

Silver particles make a covalent bond with the carboxylate component of polyether urethane when electroless-depositing silver on polyether urethane (Gray et al. 2005). Similarly, nickel and/or nickel-phosphorous chemically interact with the curing aluminium filled epoxy resin to form a covalent bond because the epoxy resin has some reactive group like hydroxyl (Omrani et al., 2008b). Actually, the hydroxyl groups in epoxy resin develops a strong adhesion to metal (Rouw 1998, Roche et al. 2002, Meiser et al. 2010, Semoto et al. 2012, Brand et al. 2004, Kahraman et al. 2008, Zapunnaya et al., 2006).

The adhesion strength will be seriously affected if water gets into the nickel-phosphorous layer. Hence the surface of the nickel-phosphorous layer on the RP model (which is used as a casting pattern) must be well dried before implanting into the aluminium filled epoxy resin so as to minimize the chance of affecting the adhesion of the layer. In fact, the cavity insert in

the mould is for low volume production, so it will not have sufficient time for water to chemically attack the interface even if it has such defects in the cavity insert. However, in case the cavity insert are to be stored for a long time, then care has to be taken to avoid water getting into the nickel-phosphorous layer.

7.8 Mould Fabrication

There are many factors to consider in practical injection mould design such as incorporation of a suitable venting system, runner system, landing zone and gates. Besides the ejection system and the water lines, most of the features are included in the injection mould used in this research. A vent of 20μm depth and 3mm width was machined on the parting surface to release the air inside the cavity.

The ejection system was eliminated from the injection mould for simplicity in this investigation. The factors affecting the de-moulding are surface roughness (smoothness) of cavity, part draft angle, resin materials property and injection temperature. A large draft angle of 4˚ is introduced in the plastic part to compensate for the absence of an ejection system. Furthermore, the nickel-phosphorous alloy layer also helps to reduce the friction between the cavity and the casting. The water lines for mould cooling are also eliminated for further simplification. This builds up stress and causes warping of the moulded part due to the non-uniform cooling rate, especially for plastic parts with thin wall thickness. This warping can be minimized by adjusting the injection moulding processing conditions.

7.9 Cost and Time for Tooling

Material costs and manufacturing costs are two major components to consider in the product development process. The cost of manufacturing the injection mould by this approach is greatly reduced since expensive machining processes are avoided. In fact, the cost of the materials such as aluminium powders, epoxy resin, RP materials and chemicals for electroless plating is low. Even though the chemical palladium chloride is relatively expensive (palladium is a noble metal), it just needs a few drops for plating the casting pattern so it is ultimately also less cost per mould. Hence, the cost of building a mould using the method outlined in this research is much lower than that of a mould made of steel. The approximate average cost for building the moulds in this research is listed in Table 12.

On the other hand, because both timely processes of machining and electric discharging are eliminated during the mould making process, the tooling preparation time is also greatly shortened. It takes less than 48 hours to complete the injection mould for moulding the plastic sample parts in this research. Therefore, the proposed rapid tooling approach yields a fast and easy method to build a mould for plastic parts at low to medium production volume. However, it should be noted that currently these are very simple moulds with no ejection, water lines, slides or inserts. It has yet to be determined how more complex parts can be manufactured using this method and the subsequent time and cost implications.

Table 12: Average costs of injection mould built by the proposed approach

Process	Time (hr.)	Cost (NZD)	Materials	Remarks
CAD Model	2	$40		Labor $20/hr.
RP Model	2	$20	R5	1 hr. labor, Perfactory machine
Pre-treatment	1	$20	Pd/Sn/Cr…	Small amount of materials is used
Electroless plating	2	$40	$NiSO_4$ $NaHPO_2$ etc.	Plating rate=10μm/hr. Layer thickness=10μm. Given extra 1 hr. for preparation and if solution decomposes.
Epoxy hardener System	1	$20	Epoxy, Al, hardener	
Slow Curing	24			Rapid tooling curing Epoxy+hardner+Al+electroless nickel plated R5 model implanted
Finishing of cavity insert	2	$40		Lathe and milling machine
Remove casting pattern	1	$20		
Assembling to injection moulding machine	1	$20		BOY 35 injection moulding machine
Mould base	4	$80		
Total (Approximately)	44	$500		

Chapter 8: Conclusion and Recommendations for Future Work

8.1 Conclusion

Competition in the injection moulding industry requires parts to be developed and produced at low cost and in less time. New technologies such as Rapid Prototyping and Rapid Tooling are being widely researched and developed to assist both product development and manufacture. Cost effectiveness and shortening the time to market are the two major motivators for the recent developments. In this research the objective was to develop a rapid soft tool process for plastic injection moulding for low volume injection moulding production. The research focussed on small parts with high definition produced using the Perfactory RP process. The aim was to use the Perfactory RP model directly in the soft tool process such that an injection mould cavity could be produced and used to manufacture several hundred parts before mould failure. The final method chosen was to electroless plate the RP model in a nickel-phosphorous layer and imbeds it in an aluminium epoxy cavity. Mechanically remove the RP model to leave a female nickel phosphorous moulding the cavity. The finished aluminium epoxy cavity with imbedded nickel-phosphorous female mould was then inserted in a base mould. Finally, polyurethane parts were then produced using a commercial injection moulding machine.

In this study it was shown that Perfactory PR photopolymer material, R5 can be nickel plated using electroless plating techniques with hypophosphite as a reducing agent. The results show that the layer actually consists of not only nickel but also phosphorous which yields better properties such as lubrication and wear resistance making it suitable as a tool for injection

moulding. Cracks and bubble free surface are obtained after carefully plating with appropriate chemical agents and bath conditions. Morphology study reveals that the nickel-phosphorous layer is uniform in thickness and there is homogeneous elemental distribution on the surface. Furthermore, the optical microscope images show there is no significant effect on dimensions of the final cavity insert after electroless nickel plating.

Application of the nickel-phosphorous layer on to the cavity insert, which is made by aluminium filled epoxy resin, improves the hardness of the tool and enhances its performance. Bond strength is the combined effect of mechanical interlocking and chemical bond between the resin matrix and nickel–phosphorous layer. Such a high adhesion resists injection flow shear thus improving the life of the tool.

It has also demonstrated that the aluminium filled epoxy cavity insert works without a cooling channel system when running the injection moulding at 170˚C. This shows that the cavity insert can operate on the injection moulding machine efficiently with reduced injection moulding cycle time. This is due to the embedded aluminium powder in the epoxy resin which increases the thermal conductivity. In contrast, conventional hard tool requires a longer time to cool down the mould which results in a long cycle time. Furthermore, this rapid cooling characteristic of aluminium filled epoxy resin also simplifies the design and fabrication of the cavity insert for the injection mould.

Injection moulding experiments conducted using the injection moulding machine in this research also demonstrates that care needs to be taken when selecting materials for the cavity insert. Special attention is needed to be paid to the injection pressure to ensure that it does not fail at certain pressure conditions. In addition, mould release agent and/or a suitable draft angle must be included for production.

Although durability of the aluminium filled epoxy resin made cavity insert is sensitive to injection pressure, the resin has a glass transition temperature of about 80˚C. However, it can withstand a melt temperature over 170˚C because of its high thermal conductivity. The heat of the melt in the cavity is quickly removed during both injection and holding phase. The mould built by this rapid tooling approach is capable of producing more than 600 plastic parts by injection moulding without wear on the cavity insert surfaces.

Finally, the research has shown it is possible to use Perfactory RP models with electroless nickel plating as a casting pattern to build a cavity insert with aluminium filled epoxy. This form of rapid tooling has been shown to work well for low volume production of plastic parts with fine features. Furthermore, the tool life is sufficient for intermediate production volume of injection moulded parts.

8.2 Recommendations for Future Work

Besides the conclusions that have been made regarding the rapid tooling method developed for low volume injection moulding of plastic, there are a number of avenues that can be explored for future work. In particular, it will be interesting to examine adhesion strength between the aluminium filled epoxy resin and nickel–phosphorous layer. The main contribution significantly influencing the mechanical interlocking is the surface roughness of the nickel–phosphorous layer. Further investigation of chemical bonds and how it influences the bonding between these two materials will be helpful to predict life of the tool under injection moulding.

It is noted that the tool is developed for low volume production of injection moulding. It is envisaged that the device will also capable for intermediate production volume. This may require using different epoxy resins and hardeners which have better thermal and mechanical properties than the one used here. Moreover, an attempt shall be made to modify the nickel–phosphorous layer, resin materials, fillers and design so that the cavity insert can endure higher injection pressure. For example, heat treating the modified insert at 300˚C for 1 hour could convert the amorphous state nickel–phosphorous layer into a crystalline state.

Finally, there are many process parameters in electroless nickel plating that affect the properties of the nickel–phosphorous layer. It will be beneficial to investigate how the bath plating parameters and substrate surface properties influence the nickel–phosphorous deposition on the RP polymer material. In addition, the electroless plating process can be further exploited in rapid prototyping and rapid manufacturing to build decorative and functional parts. A nickel–phosphorous alloy layer actually lends many remarkable properties which can be used in many industrial applications.

References

Alexandre, G., Berthelot, T., Viel, P., Mesnage, A., Jegou, P., Nekelson, F., and Palacin, S. 2010, "ABS polymer electroless plating through a one-step poly acrylic acid covalent grafting", *Applied Materials & Interfaces*, Vol. 2 No. 4, pp. 1177-1183

Alirezaei, S., Monirvaghefi, S. M., Salehi, M. and Saatchi, A., 2007, "Wear behaviour of Ni-P and Ni-P-Al_2O_3 electroless coating", *Wear*, Vol. 262, pp. 978-985

Antonio, J. P., Queiros, M. P., Martinho, P. G., Bartolo, P. J. and Antonio, S. P., 2010, "Experimental assessment of hybrid mould performance", *International Journal of Advanced Manufacturing Technology*, Vol. 50, pp. 441-448

Balaraju, J. N., Jahan, S. M., Jain, A. and Rajam, K. S., 2007(a), "Structure and phase transformation behaviour of electroless Ni-P alloys containing tin and tungsten", *Journal of Alloys and Compounds*, Vol. 436, pp. 319-327

Bjorneklett, A., Halbo, L. and Kristiansen H, 1992, "Thermal conductivity of epoxy adhesives filled with silver particles", *International Journal of Adhesion and Adhesives*, Vol. 12, No. 2, pp. 99-104

Bozzini, B., Martini, C., Cavallotti, P. L. and Lanzoni, E., 1999, "Relationships among crystallographic structure, mechanical properties and tribological behaviour of electroless Ni-P (9%)/ B_4C films", *Wear*, Vol. 225-229, pp. 806-813

Brand, J. V., Gils, S. V., Beentjes, P. C. J., Terryn, H., Sivel, V. and De Wit, J. H. W., 2004, "Improving the adhesion between epoxy and aluminium substrates", *Progress in Organic Coatings*, Vol. 51, pp. 339-350

Brostow, M., Dutta, M. and Rusek P, 2010, "Modified epoxy coatings on mild steel: Tribology and surface energy"; *European Polymer Journal*, Vol. 46, pp. 2181-2189

Bulasara, V. K., Chandrashekar, O. and Uppaluri, R., 2011(a), "Effect of surface roughness and mass transfer enhancement on the performance characteristics of nickel-hypophosphite electroless plating baths for metal-ceramic composite membrane fabrication", C*hemical Engineering Research and Design*, Vol. 89 , pp. 2485-2494

Bulasara, V. K., Thakuria, H., Uppaluri, R. and Purkait, M. K., 2011(b), "Effect of process parameters on electroless plating and nickel-ceramic composite membrane characteristics", *Desalination*, Vol. 268, pp. 195-203

Chang, Y., Duh, J. and Chen Y, 2001, "Fabrication and crystallization behaviours of sputtered Ni-Cu-P films on tool steel", *Surface & Coating Technology*, Vol. 139, pp. 233-243

Cheah, C. M., Chua, C. K. and Ong, H. S., 2002, "Rapid Moulding using epoxy Tooling Resin", *The International Journal of Advanced Manufacturing Technology*, Vol. 20, pp. 368-374

Cheng, Y. H., Zou, Y., Cheng, L. and Liu W, 2009, "Effect of the microstructure on the properties of Ni-P deposits on heat transfer surface", *Surface & Coating Technology*, Vol. 203, pp. 1559-1564

Cheon, S., Park, S., Rhym, Y., Kim, D. and Lee J, 2011, "The effect of bath conditions on the electroless nickel plating on the porous carbon substrate", *Current Applied Physics*, Vol. 11, pp. 790-793

Chung, S. M. and Yap, A. U. J., 2005, "Effect of surface finish on indentation modulus & hardness of dental composite restoratives", *Dental Material*, Vol. 21, pp. 1008-1016.

Deng, S., Hou, M. and Ye, L., 2007, "Temperature-dependent elastic moduli of epoxies measured by DMA and their correlations to mechanical testing data", *Polymer Testing*, Vol. 26, pp. 803-813

Derek, K., 2009, "Nano technology improves insert coating adhesion", *Modern Machine Shop*, Vol. Jan 2009, pp.81-84.

Di, L., Liu, B., Song, J., Dan, S. and Yang, D., 2011, "Effect of chemical etching on the Cu/Ni metallization of poly (ether ether ketone) / carbon fibre composites", *Applied Surface Science*, Vol. 257, pp. 4272-4277

Ding, Y., Lan, H., Hong, J. and Wu, D., 2003, "An integrated manufacturing system for rapid tooling based on rapid prototyping", *Robotics and Computer-Integrated Manufacturing*, Vol. 20, pp. 281-288

Dvorak, P., 1998, "Here comes rapid tooling", *Machine Design*, Vol. 70, No. 13

EnvisionTEC, 2012, www.envisiontec.com (Accessed 14-06-2012)

Ferreira, J. C., 2004, "Manufacturing core-boxes for foundry with rapid tooling technology", *Journal of Materials Processing Technology*, Vol. 155-156, pp. 1118-1123

Ferreira, J. C. and Mateus, A., 2000, "Studies of rapid soft tooling with conformal channels for plastic injection moulding", *Journal of Materials Processing Technology*, Vol. 142, pp. 508-516

Francis, E. H. and Haider, E. A., 2000, "Laser sintered rapid tools with improved surface finish and strength using plating technology", *Journal of Materials Processing Technology*", Vol. 121, pp. 318-322

Furukawa, S. and Mehregany, M., 1996, "Electroless plating of nickel on silicon for fabrication of high-aspect-ratio microstructures", *Sensors and Actuators*, Vol. 56, pp. 261-266

Gibbons, G. J. and Hansell, R. G., 2005, "Direct tool steel injection mould inserts through the Arcam EBM free-form fabrication process", *Assembly Automation*, Vol. 25, No. 4, pp. 300-305

Goyanes, S., Rubiolo, G., Marzocca, A., Salgueiro, W., Somoza, A., Consolati, G. and Mondragon, I., 2003, "Yield and internal stress in aluminium filled epoxy resin: a compression test and positron annihilation analysis", *Polymer*, Vol. 44, pp. 3193-3199

Gray, J. E., Norton, P. R. and Griffiths, K., 2005, "Mechanism of adhesion of electroless-deposited silver on poly(ether urethane)",*Thin Solid Films*, Vol. 484 , pp. 196-207

Griffiths, C. A., Dimov, S. S., Brousseau, E. B. and Hoyle, R. T., 2007, "The effects of tool surface quality in micro-injection moulding", *Journal of Materials Processing Technology*, Vol. 189,pp. 418-427

Griffiths, C. A., Dimov, S. S., Fischer, S., Spitzbart, M. and Lacan, F., 2013(a), "Micro-stereolithography tools for small-batch manufacture of polymer micro-parts", *Journal of Engineering Manufacture*, Vol. 226, Part B

Gu, H. and Shulkin, B., 2000, "Important of processing temperature control in laser beam hardening of production dies", Stronach Centre for Innovation, #903

Harris, R. A., Newlyn, H. A., Hague, R. J. M. and Dickens, P. M., 2003, "Part shrinkage anomalies from Stereolithography injection mould tooling", *International Journal of Machine Tools and Manufacturing*, Vol. 43, pp. 879-889

Harris, R.A., Newlyn, H. A. and Dickens, P. M., 2002(b), "Selection of mould design variables in direct steriolithography injection moulding tooling", *Institute of Mechanical Engineers*, Vol. 216, No. 4,pp. 499-505

Hassan, A., Rahman, A. N. and Yahya, R., 2011, "Extrusion and injection moulding of glass fibre/MAPP/polypropylene: effect of coupling agent on DSC, DMA, and mechanical properties"; *Journal of Reinforced Plastics & Composites*, Vol. 30, No. 14, pp. 1223-1232

Hilton, P.D., 2000, "Rapid Tooling Technologies and Industrial Applications", Marcel Dekker Inc, New York US

Hopkinson, N. and Dickens, P, 2000, "A comparison between stereolithography and aluminium injection moulding tooling", *Rapid Prototyping Journal*, Vol. 6, No. 4, pp. 253-258

Jacobs, P. F., 1992, Rapid Prototyping and Manufacturing: Fundamentals of Stereolithography. Dearborn: Society of Manufacturing Engineering

Jorgensen, T. H., 2001, "Case study: Epoxy tooling speeds time to market", www.danish technologicalinstitute.com, (Accessed on 20-03-2013)

Kahraman, R., Sunar, M. and Yilbas, B., 2008,"Influence of adhesive thickness and filler content on the mechanical performance of aluminium single-lap joints bonded with aluminium powder filled epoxy adhesive", *Journal of Materials Processing Technology*, Vol. 205, pp.183-189

Kantola, K. and Ekebom, L., 2000, "Modelling and controlling of electroless nickel plating process",

Karalekas, D. and Ntoniou, K.., 2004, "Composite rapid prototype: overcoming the drawback of poor mechanical properties", *Journal of Materials Processing Technology*, Vol. 153-154, pp.526-530.

Karalekas, D. E., 2003(b), "Study of mechanical property of nonwoven fibre mat reinforced photopolymer used in rapid prototyping", *Materials & Design*, Vol. 24, pp. 665-670.

Keong, K. G., Sha, W. and Malinov, S., 2003, "Hardness evaluation of electroless nickel-phosphorus deposits with thermal processing", *Surface & Coating Technology*, Vol. 168, pp. 263-274

Kilik, R. and Davies, R., 1989(a), "Mechanical properties of adhesive filled with metal powder", *International Journal of Adhesion and Adhesives*, Vol. 9, No. 4, pp. 224-228

Kilik, R., Davies, R. and Darwish, S. M. H., 1989(b), "Thermal conductivity of adhesive filled with metal powders", *International Journal of Adhesion and Adhesives*, Vol. 9, No. 4, pp. 219-223

Kim, G. M., Qin, H., Fang, X., Sun, F. C. and Mather, P. T., 2003, "Hybrid Epoxy-Base Thermosets Base on Polyhedral Oligosilsesquioxane: Cure Behaviour and Toughening Mechanisms", *Journal of Polymer Science, Part B*, Vol. 41, pp. 3299-3313

Kim, K. D., Yang, D. Y. and Jeong, J. H., 2006, "Plaster casting process for prototyping of die casting based on rapid tooling", *International Journal of Advanced Manufacturing Technology*, Vol. 28, pp. 923-929

Kovacs, J. G., Kortelyesi, G., Kovacs, N. K. and Suplicz, A., 2011, "Evaluation of measured and calculated thermal parameters of a photopolymer", *International Communications in Heat and Mass Transfer*, Vol. 38, pp. 863-867

Krumova, M., Klingshirn, C., Haupert, F. and Friedrich, K., 2001, "Microhardness studies on functionally graded polymer composites"; *Composites Science and Technology*, Vol. 61, pp. 557-563

Lencina, D. C., Ahrens, C. H., Salmoria, G. V. and Lafratta, F. H., 2007, "Injection moulding of PA 6.6 in Stereolithography moulds coated with electroless Ni-P", *Polymerose,* Vol. 17, No. 2, pp. 88-92

Leon, C., Ochoa, E. G., Guerra, J. G. and Sanchez, J. G., 2010, "Annealing temperature effect on the corrosion parameters of auto catalytically produced Ni-P and Ni-P-Al_2O_3 coating in artificial seawater", *Surface & Coating Technology*, Vol. 205, pp. 2425-2431

Lewis, D. B.and Marshall, G. W., 1996, "Investigation into the structure of electrodeposited nickel-phosphorus alloy deposits", *Surface & Coating Technology*, Vol. 78, pp. 150-156

Li, L. and Liu, B., 2011, "Study of Ni-catalyst for electroless Ni-P deposition on glass fibre", *Materials Chemistry and Physics*, Vol. 128, pp. 303-310

Lin, J. F., Lian, J. C. and Li, K. Y., 1997, "The effect of electroless nickel film on the Tribological characteristics of alumina coating", *Wear*, Vol. 209, pp. 199-212

Liu, Z. and Gao, W., 2006(a), "Electroless nickel plating on AZ91 Mg alloy substrate", *Surface & Coating Technology*, Vol. 200, pp. 5087-5093

Liu, Z. and Gao, W., 2006(b), "The effect of substrate on the electroless nickel plating of Mg and Mg alloys", *Surface &Coating Technology*, Vol. 200, pp. 3553-3560

Lu, G. and Zangari, G., 2002, "Corrosion resistance of ternary Ni-P based alloys in sulphuric acid solution", *Electrochemica Acta*, Vol. 47, pp. 2969-2979

Luan, B., Yeung, M., Wells, W. and Liu, X., 2000, "Chemical surface preparation for metallization of Stereolithography polymer", *Applied surface science*, Vol. 156, pp. 26-38

Ma, S., Gibson, I., Balaji, G. and Hu, Q.J., 2007, "Development of epoxy composites for rapid tooling applications", *Journal of Materials Processing Technology*, Vol. 192-193, pp. 75-82

Malecki, A. and Ilnicka, M., 2000, "Electroless nickel plating from acid bath", *Surface & Coating Technology*, Vol. 123, pp. 72-77

Meiser, A., Kubel, C., Schafer, H. and Possart, W., 2010, "Electron microscopic studies on the diffusion of metal ions in epoxy-metal interface, International", *Journal of Adhesion & Adhesives*, Vol. 30, pp. 170-177

Miller, B., 1997, "Injection molds 'to go' No, but lead time is dropping fast", *Plastics World*, Vol. 55, No. 4, pp. 38-42

Mori, K., Hirahara, H. and Oishi, Y., 1997, "Direct Adhesion between Electroless Nickel-P plated metals and NBR compounds during curing", *Rubber Chemistry and Technology*, Vol. 70, No. 2, pp. 211-221

Nagahanumaiah and Ravi, B., 2008, "Effect of injection moulding parameters on shrinkage and weight of plastic part produced by DMLS mould", *Rapid Prototyping Journal*, Vol. 15, No. 3, pp. 179-186

Omrani, A., Simon, L. C., Rostami, A.A. and Ghaemy, M., 2008(b), "Study on curing mechanism of DGEBA/nickel-imidazole system", *Thermochemica Acta*, Vol. 468, pp. 39-48

Palmer, A. E. and Colton, J. S., 2000, "Failure mechanisms in Stereolithography injection moulding tools", *Polymer Engineering and Science*, Vol. 40, No. 6

Perkins, W. G., 1999, "Polymer toughness and impact resistance", *Polymer Engineering and Science*, Vol. 39, No. 12, pp. 2445-12460

Possart, G., Presser, M., Passlack, S., Geib, P. L., Kopnarski, M., Brodyanski, A. and Steinmann, P., 2009, "Micro-macro characterisation of DGEBA-based epoxies as a preliminary to polymer inter phase modelling", *International Journal of Adhesion & Adhesives*, Vol. 29, pp. 478-487

Qin, W., Long, J. and Liu, F., 2010, "Improvement on hardness of 6061 Al alloy using an electroless Ni-P coating", *Applied Mechanics and Materials*, Vol. 26-28, pp. 293-296

Rahmati, S. and Dickens, P., 2007, "Rapid tooling analysis of Stereo lithography injection moulding tooling", *International Journal of Machine Tools & Manufacture- Design, Research and Application*, Vol. 47, pp. 740-747

Roche, A. A., Bouchet, J. and Bentadjine, S., 2002, "Formation of epoxy-diamine/metal interfaces", *International Journal of Adhesion & Adhesives*, Vol. 22, pp. 431-441

Rodet, V. and Colton, J. S., 2003, "Properties of rapid prototype injection mould tooling materials", *Polymer Engineering and Science*, Vol. 43, No. 1, pp. 125-137

Rossi, S., Deflorian, F. and Venturini, F., 2004, "Improvement of surface finishing and corrosion resistance of prototypes produced by direct metal laser sintering", *Journal of Materials Processing Technology*, Vol. 148, pp. 301-309

Rouw, A. C., 1998, "Model epoxy powder coating and their adhesion to steel", *Progress in Organic Coatings*, Vol. 34, pp. 181-192

Roy, S. and Sahoo, P., 2010, "Optimization of multiple roughness characteristics of chemically deposited Ni-P-W coating using weighted principal component analysis", Jadavpur University, Kolkata

Sadegh, R., Reza, R. M. and Javad, A., 2009, "Design and manufacture of a wax injection tool for investment casting using rapid tooling", *Tsinghua Science and Technology*, Vol. 14, No. S1, pp. 108-115

Semoto, T., Tsuji, Y. and Yoshizawa, K., 2012, "Molecular understanding of the adhesive force between a metal oxide surface and an epoxy resin: effects of surface water", *Bull Chemistry Society of Japan*, Vol. 85, No. 6, pp. 672-678

Steven, A., 1997, "From CAD art to rapid metal tools", *Mechanical Engineering ProQuest*, Vol. 119, No. 3

Sugihara, S., Okada, S., Ohtsuka, H. and Yamaki, J., 1996, "Effect of the surface state of plastics on adhesive strength in electroless plating", *Journal of Applied Polymer Science*, Vol. 59, pp. 1751-1758

Tang, X., Wang, J., Wang, C. and Shen, B., 2011, "A novel surface activation method for Ni/Au electroless plating of acrylonitrile-butadiene-styrene", *Surface & Coating Technology*, Vol. 206, pp. 1382-1388

Tang, X., Cao, M., Bi, C., Yan, L. and Zhang, B., 2008, "Research on a new surface activation process for electroless plating on ABS plastic", *Material Letters*, Vol. 62, pp. 1089-1091

Tomori, T., Melkote, S. and Kotnis, M., 2004, "Injection mould performance of machined ceramic filled epoxy tooling boards", *Journal of Materials Processing Technology*, Vol. 145, pp. 126-133

Vasconcelos, P., Lino, F. J., Baptista, A. M. and Neto, R. J. L., 2006, "Tribological behaviour of epoxy based composites for rapid tooling", *Wear*, Vol. 260, pp. 30-39

Vasconcelos, P. V., Lino, F. J., Magalhaes, A. and Neto, R. J. L., 2005, "Impact fracture study of epoxy-based composites with aluminium particles and milled fibres", *Journal of Materials Processing Technology*, Vol. 170, pp. 277-283

Vojdani, M., Bagheri, R. and Khaledi, A. A. R., 2012, "Effects of aluminium oxide addition on the flexural strength, surface hardness, and roughness of heat polymerised acrylic resin", *Journal of Dental Sciences*, pp. 1-7

Wai, S. W., Spinks, G. M., Brown, H. R. and Swain, M., 2004, "Surface roughness: its implications and inference with regards to micro indentation measurements of polymer mechanical properties", *Polymer Testing*, Vol. 23, pp. 501-507

Waris, T. F., Turunen, M. P. K., Laurila, T. and Kivilahti, 2005, "Evaluation of electrolessly deposited NiP integral resistors on flexible polyimide substrate", *Microelectronics Reliability*, Vol. 45, pp. 665-673

West System, 2012, www.westsystem.com (Accessed on 10-02-2012)

Wu, F., Tien, S., Duh, J., Wang, J., 2003, "Surface characteristics of electroless and sputtered Ni-P-W alloy coatings", *Surface & Coatings Technology*, Vol. 166, pp. 60-66

Wu, Y., Liu, H., Shen, B., Liu, L. and Hu, W., 2006, "The friction and wear of electroless Ni-P matrix with PTFE and/or SiC particles composite", *Tribology International*, Vol. 39, pp. 553-559

Xie, Z., Yu, G., Hu, B., Lei, X., Li, T. and Zhang, J., 2011, "Effect of $(NH_4)_2SO_4$ on the characteristics of the deposits and properties of an electroless Ni-P plating solution", *Applied Surface Science*, Vol. 257, pp. 5025-5031

Zapunnaya, K. V., Lipatov, S., Todosiichuk, T. T., Yashchenko, L. N.,
Krivchenko, G. N. and Gorbatenko, A.N., 2006, "Influence of the kinetics of curing of epoxyurethane adhesives on the strength of joints", *International Polymer Science and Technology*, Vol. 33, No. 11, pp. 16-20

Zhang, Q., Wu, M. and Zhao, W., 2005, "Electroless nickel plating on hollow glass microspheres", *Surface & Coating Technology*, Vol. 192, pp. 213-219

Zhao, Q., Liu, Y. and Abel, E. W., 2005, "Surface free energies of electroless Ni-P based composite coatings", *Applied Surface Science*, Vol. 240, pp. 441-451

Zhao, Q., Liu, Y., Steinhagen, H. M. and Liu, G., 2000, "Graded Ni-P-PTFE coatings and their potential applications", *Surface &Coating Technology*, Vol. 155, pp. 279-284

Zhao, S., Schadler, L. S., Duncan, R., Hillborg, H. and Auletta, T., 2008, "Mechanism leading to improved mechanical performance in nano scale alumina filled epoxy", *Composites Science and Technology*, Vol. 68, pp. 2965-2975